ANALYSIS OF CLOUD-FREE LINE-OF-SIGHT PROBABILITY CALCULATIONS

THESIS

Joseph J. Golemboski III, Capt, USAF

AFIT/GM/ENP/01M-03

DEPARTMENT OF THE AIR FORCE
AIR UNIVERSITY

AIR FORCE INSTITUTE OF TECHNOLOGY

Wright-Patterson Air Force Base, Ohio

AFIT/GM/ENP/01M-03

ANALYSIS OF CLOUD-FREE LINE-OF SIGHT PROBABILITY CALCULATIONS

THESIS

Presented to the Faculty of the Graduate School of Engineering

of the Air Force Institute of Technology

Air University

Air Education and Training Command

In Partial Fulfillment of the Requirements for the

Degree of Master of Science

Joseph J. Golemboski III, B.S.,

Captain, USAF

March 2001

AFIT/GM/ENP/01M-03

ANALYSIS OF CLOUD-FREE LINE-OF-SIGHT PROBABILITY CALCULATIONS

Joseph J. Golemboski III, B.S.,

Captain, USAF

Approved:

Michael K. Walters, Lt Col, USAF Chairman, Advisory Committee	Date
Ronald P. Lowther, Lt Col, USAF Member, Advisory Committee	Date
Raymond R. Hill, Lt Col, USAF Member, Advisory Committee	Date
Professor Daniel E. Reynolds Member, Advisory Committee	Date

Acknowledgments

I would like to express my sincere appreciation to my thesis advisor, Lieutenant Colonel Michael K. Walters, whose assistance was a great help in completing this project and my overall education. His style led me down avenues I reluctantly traveled and taught me many lessons I'll carry with me through my Air Force career. The other members of my committee, Lieutenant Colonel Ron Lowther, Lieutenant Colonel Ray Hill, and Professor Dan Reynolds were invaluable sounding boards for numerous approaches to the problem, both good and bad. I must also thank Lieutenant Colonel Mark O'Hair and the UAV Battlelab for sponsoring me and providing the resources for me to complete this task.

I am deeply indebted to the team at Phillips Laboratory, Joel Mozer, Guy Seeley, and Sara Gordon, who provided me a crash course in C-programming. Along with Capt Glenn Kerr of the 88th Weather Squadron, their assistance made it possible to process the data in a short period. Additionally, I would like to thank Capt Chris Stock of the MM5 team at AFWA, who delivered critical gridded output data to me over the holidays.

Finally, and most importantly, my deepest thanks goes to my wife and children, Without their support and understanding, I would never have made it through the long days and nights spent in the lab.

Joseph J. Golemboski III

Table of Contents Page

LIST OF FIGURES Page

LIST OF TABLES Page

Abstract

Cloud-free line-of-sight probabilities were calculated using two separate methods. The first was a variation of a method developed by the Rand Corporation in 1972. In it, CFLOS probabilities were calculated using empirical data based on five years of photograms taken over Columbia, Missouri and forecasted cloud amounts rather than climatological values. The second was a new approach using the Cloud Scene Simulation Model developed by Phillips Laboratory. Cloud scenes were generated using forecasted cloud fields, meteorological inputs, and thirty random numbers. Water content files were produced and processed through a follow-on program to determine the extinction coefficients at each grid point in the working domain. A reiterative routine was written to integrate the extinction coefficients along a view angle from the top of the domain down to the surface at separate points within the horizontal domain. The values of each point were summed and averaged over the working domain to determine the CFLOS probability for the target area.

The nadir look angle was then examined for both methods. Stratus, stratocumulus, cumulus, and altocumulus cloud types were independently examined with the CSSM generated cloud scenes. Each method and cloud type were compared against the known CFLOS probability for nadir.

Results indicate the method developed in 1972 underestimates CFLOS probabilities by as much as twelve per cent with horizontal cloud coverage ranging from 30 to 80 per cent. CSSM generated cloud scenes varied depending on the cloud type analyzed, with stratocumulus clouds measuring up the best against the known probabilities.

METHODS DETERMINING CLOUD-FREE LINE-OF-SIGHT PROBABILITIES USING THE PHILLIPS LABORATORY CLOUD SCENE SIMULATION MODEL AND THE FIFTH GENERATION MESOSCALE MODEL

I. Introduction

1.1 Background

Cloud-free line-of-sight (CFLOS) probabilities are tactical decision aids designed to assist combat aircraft in putting bombs, precision-guided munitions, or even cameras, on target. When aircraft fly at altitudes greater than 5,000 feet, the presence of clouds between aircraft and the ground target can seriously diminish the chance for mission success (Air Weather Service 1992). CFLOS probabilities are usually expressed as a percentage between 0 and 100. Often times CFLOS probabilities are mistakenly interpreted as how much of the surface is visible at altitude. A CFLOS probability of 60 per cent actually means that if the same cloud conditions were present over an infinite amount of times, the target would be visible 60 percent of the time.

1.2 Importance of the Research

Cloud cover has a tremendous impact on all aspects of reconnaissance and surveillance missions. Satellites and high-altitude reconnaissance aircraft have carried the bulk of these missions, but they could not mitigate the presence of clouds over the target area. A new breed of reconnaissance aircraft, unmanned aerial vehicles (UAVs),

are entering service, bringing more options for prosecuting targets. The current Air Force medium altitude endurance (MAE) UAV, Predator, can loiter in hostile areas at lower altitudes while eliminating the risk to human life. However, this luxury does have a monetary price tag if the Predator is shot down. The need for the information gathered must outweigh the expense of the aircraft. Factors to consider are the priority of the target, threat regions, weather impinging on the aircraft, and the ability to actually "see" the ground.

With everything UAVs offer, they are still hampered by some significant limitations. Due to the absence of pilots on-board, MAE/UAVs must fly in assigned altitude blocks in order to deconflict with other "manned" aircraft. Air vehicle operators (AVOs) and imagery specialists view the scene through a two-dimensional screen. They cannot efficiently maneuver into breaks in the clouds to see through. While weather personnel will never be able to accurately forecast the presence of clouds over small areas, they can produce a forecasted distribution of clouds at multiple levels over slightly larger areas. Advancements in cloud simulation models have made it possible to input cloud distribution parameters and generate realistic and plausible cloud scenes. CFLOS probabilities can then be calculated, providing the decision-makers some idea on the degree of success for a mission.

1.3 Statement of the Problem

In general, cloud-free line-of-sight probabilities are calculated for strategic assets, which include upper-atmosphere and space-based vehicles. For strategic considerations,

CFLOS probabilities are calculated using climatic data for the distribution of clouds. Reconnaissance assets flying at the top of the atmosphere (U-2) have CFLOS probabilities based on "looking" through the entire cloud scene. What about those assets cruising in and between the cloud layers themselves? How can a realistic CFLOS value be created for those missions?

Advancements in computer technology have opened the way to better atmospheric modeling. Models, such as the fifth-generation mesoscale model (MM5), can produce forecasts out to seventy-two hours and up to four times a day in many areas of the world depending on resource limitations. Meteograms display the horizontal and vertical distribution of clouds, two key ingredients for CFLOS calculations. However, can a cloud simulation model be used to produce realistic probabilities required to influence a mission commander's decision on which targets to prosecute?

1.4 Benefit from Solving the Problem

CFLOS probabilities calculated from simulated cloud scenes should be beneficial for the low to mid-altitude aircraft by removing extraneous clouds from the equation. That is, CFLOS probabilities for an aircraft at 15,000 feet high will not consider the clouds at 20,000 feet in the calculations. Mission planners would be able to minimize the impact of clouds in the area by planning the routes accordingly. Additionally, the probabilities can be updated as the forecast changes, allowing for a dynamic re-tasking of targets.

1.5 Research Objective

This thesis is a proof of concept in calculating cloud-free lines-of-sight probabilities for various altitudes, view angles, and cloud amounts. It compares the results of a modified method developed by Rapp, Schutz, and Rodriguez of the Rand Corporation with a new approach using the Cloud Scene Simulation Model (CSSM).

CFLOS probabilities are an objective means of determining the consequences of clouds. For example, a mission planner receives a forecast for broken clouds over the target area and must try to interpolate how those clouds will hinder a mission. A CFLOS probability along with the cloud forecast would provide the mission planner a clearer picture on the significance of the clouds. The goal of this research is to begin developing a dynamic approach to CFLOS probability calculations based on observed/forecasted cloud cover instead of climatology.

1.6 Procedure

CFLOS probabilities were calculated by using analyzed data from MM5 meteogram forecasts and gridded output data as inputs to the two schemes. Chapter 3 provides a detailed description of the process. The following briefly outlines steps taken to conduct the study.

1.6.1 MM5

The MM5 ran at AFWA produces forecasts valid every three hours out to the seventy-two hour point and is run four times a day (00, 06, 12, and 18 UTC).

Meteograms and gridded output data for Sarajevo were subjectively analyzed to determine cloud bases, tops, types, and horizontal distribution.

1.6.2 Rapp, Schutz, and Rodriguez

Once again, data from the meteograms were used as inputs for the procedure developed by Rapp, Schutz, and Rodriguez. Background information and a description of the process are detailed in sections 2.3 and 3.2, respectively.

1.63 Cloud Scene Simulation Model

The CSSM developed by Phillips Laboratories was used for the new CFLOS approach. Data from the aforementioned MM5 were converted into an input file. A cloud scene was generated and a solar extinction program was used to determine the presence of clouds from altitude down to the ground for a given look angle. A Bernoulli distribution of the presence of clouds was then calculated. The process was repeated at each grid point in the domain to determine the CFLOS probability.

1.7 Thesis Organization

Chapter 2 presents a synopsis of all the information in the literature having a bearing on the problem. A description of the Predator UAV is provided. The MM5 and CSSM models will be described as well as the method developed by Rapp, Schutz, and Rodriguez. Chapter 3 explains the methodology used to evaluate the two schemes, while

Chapter 4 presents the results of the analysis and summarizes their meanings. Chapter 5 draws conclusions based on the data and provides recommendations for future research and operational implementation.

II. Literature Review

2.1 RQ-1A Predator

The first UAV specifically designed to meet the requirement for persistent intelligence, surveillance, and reconnaissance information is the RQ-1A Predator. Predator was the first successful Advanced Concept Technology Demonstration, a new acquisition process designed to reduce cost and development time by relying on commercial-off-the-shelf/government-off-the-shelf technology to the maximum extent possible (Air Combat Command 1998). Because Predator is a medium-altitude, long-endurance UAV, it cruises at altitudes ranging from 8,000-18,000 feet above ground level. It is equipped with a "ball" containing three different types of imaging cameras. The first is a full color day-TV. The second is also a day-TV camera, but it contains a 900-mm spotter lens for extremely close-up pictures. The last is a variable aperture infrared camera for low light/night operations. All three cameras produce full motion video. The aircraft and its sensors are all commanded through the ground control station (GCS) via C-band line-of-sight data link or a Ku-band satellite data link for beyond line-of-sight operations.

2.1.1 Physical Description

For all of its capabilities, the aircraft is rather small and lightweight (Figure 2-1). It is twenty-seven feet long and seven feet high, with a wingspan of 48.7 feet. With a full fuel load, it can weigh around 2300 pounds. The max speed is on the range of 100 knots

at level flight. Therefore, weather conditions such as thunderstorms, turbulence, and icing need to be addressed during mission planning and execution. Due to the radio-wave links to the aircraft, it must land at the location of its GCS, making weather at home station another critical aspect.

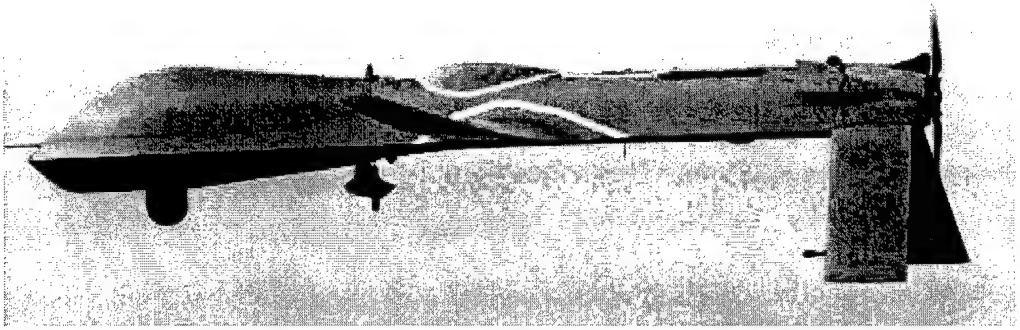

Figure 2-1. RQ-1A Predator.

2.1.2 Mission

The mission of Predator is to provide "real-time" video to on-scene commanders as well as theater mission planners. A typical mission begins with receipt of the target deck from the theater reconnaissance cell. The pilots and sensor operators plan their mission profile based on the importance of the targets, threats around the areas, time-on-target requirements, and optimization of flight time. In most cases, the aircraft will fly within three miles of a target to achieve viewing angles ranging from 45 to 90 degrees straight down. Therefore, mission success is highly dependent on the ability to monitor what the enemy is doing.

2.2 UAV Mission Routing Program Developed by AFIT

The AFIT UAV Router program developed over two years by Captain Kevin O'Rourke, Captain Garry W. Kinney Jr. and Second Lieutenant Robert W. Harder is a heuristic optimization program developed to plan Predator missions based on the following parameters: priority of target, airspace time, threat regions, flight time, ad-hoc targets, pop-up threats, no-fly zones, and assigned altitudes. The program attacks the dynamic routing problem of UAVs to re-calculate the mission route when any of the parameters changes. In order to do so, the program needs to be fast enough to be operationally effective, robust enough to handle a wide scope of problems, and reliable enough to provide optimal (or near optimal) solutions (O'Rourke 1999).

To actively adjust the tabu length based on the quality of the search, the program employs a reactive tabu heuristic. Using adaptive memory structures to search the solution space, the program makes moves from one solution to another in a forced and orderly manner. The program selects a solution from a discrete set provided the solution is not on the tabu list. The tabu list contains all the solutions previously visited. With each iteration, only new solutions are examined, forcing the program to choose the best non-tabu solution.

The AFIT Router is now ready to incorporate weather parameters to build the mission route around and adjust to weather conditions while in flight. Forecasts of thunderstorms, turbulence, and icing can be ingested into the program to build weather 'no-fly' zones. These zones could be avoided and possibly revisited to if the weather improved during the flight time. In addition to the influence of weather on the

performance of the aircraft, conditions influencing the efficiency of the cameras could also be considered. In order to provide surveillance of ground activities, the cameras require a cloud-free line-of-sight to the ground.

2.3 Cloud-Free Line-of-Sight Calculations

In order to understand how to calculate CLOS probabilities, one needs to understand the physical aspects of clouds vertically as well as horizontally. During the month of April, 1961, Air Weather Service (AWS) Special Meteorological Reconnaissance Flight and Instrument Laboratory flew a B-57 at an altitude of 40,000 feet directly over observing stations in the western United States, simultaneously taking a series of vertically oriented, overlapping photographs of the area beneath the plane (Appleman 1962). These photographs were compared to special observations taken as the aircraft passed overhead. The results of this study suggested surface observations overestimated the low cloud cover, but were in good agreement with the middle and high cloud regions. The study also concluded the presence of high cirrus permitted visual penetration in 75 per cent of the cases, and limited penetration in the remainder.

In 1965, Lt Col John T. McCabe developed a method to determine CFLOS probabilities using climatological data on clouds and sunshine. Dividing the year into two seasons, summer (May-October) and winter (November-April), McCabe compared the occurrence of "bright sunshine" with the mean observed cloud cover for 20 US stations. Assuming the occurrence of bright sunshine corresponded with a cloud-free line-of-sight, he constructed a graph (Figure 2-2) estimating the probability of CFLOS

through the whole atmosphere as a function of mean total cloud cover, solar elevation, and viewing angle. Then assuming the basic relationships among these three variables would apply for all cloud heights, McCabe devised a scheme for estimating the distribution of clouds as a function of height, based on the observations of de Bary and Möller (1963), which were made over central Europe (Rapp, Shutz, and Rodriguez 1973).

McCabe's work was one of the first to address the discrepancy between a ground observer's view of the sky and the actual cloud amount. Half of the area of the sky dome which the observer integrates to get the total sky cover is less than 30 degrees above the horizon. Thus, it is often the case where the observer's view of the sky is more blocked by the sides of the clouds than by their bases, and over a period of time, the amount of cloud overhead is much less than the cloud cover reported by the observer (McCabe 1965). Applications of McCabe's method are limited to areas of homogeneous cloudiness. For example, this method could not be applied in areas east of the Rockies where there is a higher frequency of clouds in a particular (windward) direction. For such cases it would probably be desirable to analyze two homogenous areas--one windward and one leeward.

The following year, Iver A. Lund of the Air Force Cambridge Research Laboratory described and compared five methods for estimating probabilities of clear lines-of-sight. Observations used to determine coefficients and to test the methods were taken from three separate locations: Burlington, Vermont; Bismarck, North Dakota; and San Diego, California (Lund 1966). The choice for these three stations was based on an attempt to sample considerably different cloud climatologies. Cloud cover observations were taken during the period 1951-1965.

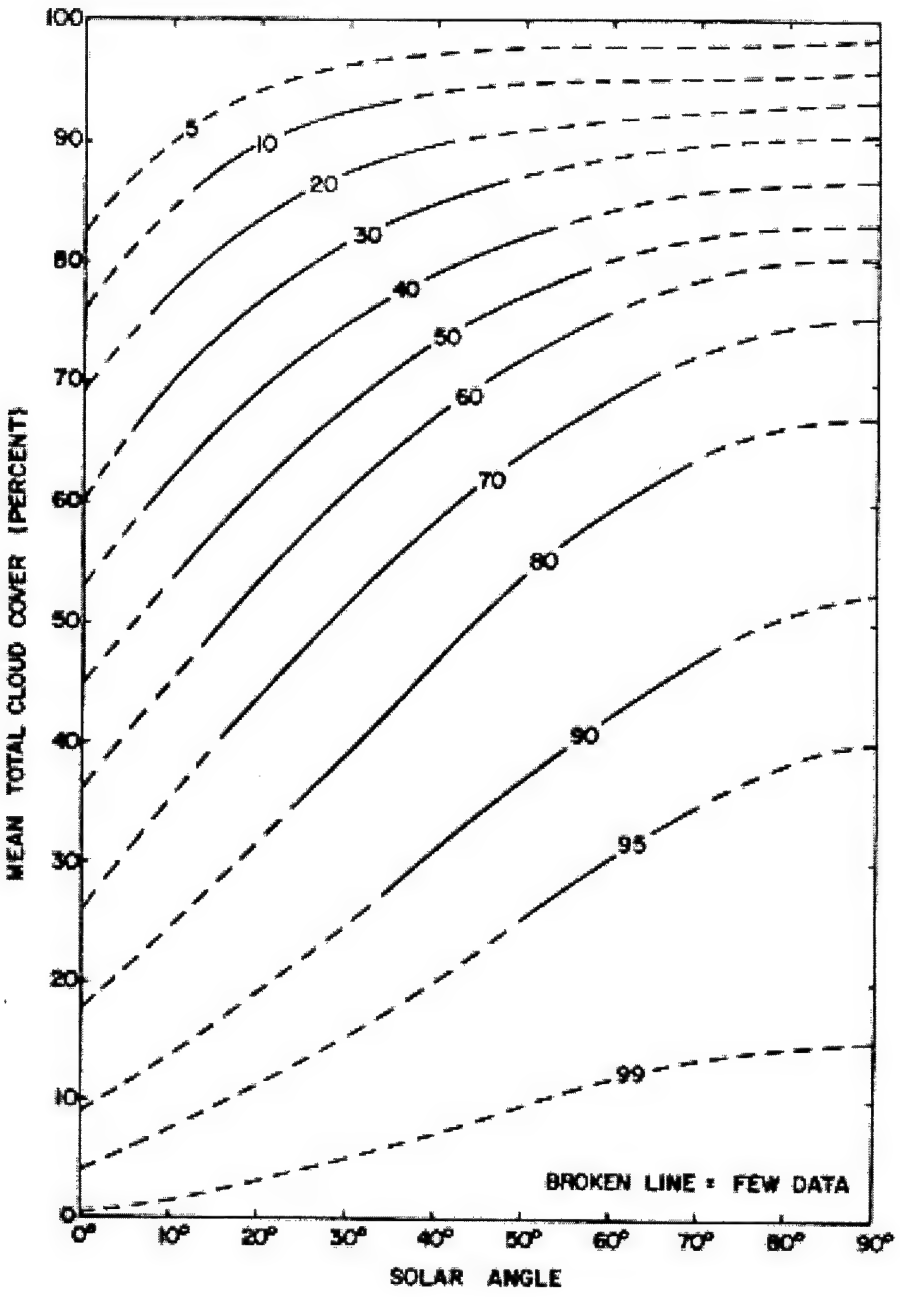

Figure 2-2. Approximate CFLOS probability as a function of cloud cover and sun angle (after McCabe, 1965).

The results of Mr. Lund's comparisons showed the McCabe method inferior to almost all other methods at first glance. However, the coefficients in the McCabe method were developed using seventeen other observation sites, rather than just the three in the comparison. Mr. Lund conceded the McCabe method should be more stable and applicable to general usage than the other methods.

The next step sought to incorporate the sky cover overestimation and view angles in a study of photograms taken from the U.S. National Weather Service (NWS) observing site at Columbia, Missouri. Photograms are high contrast photographs of the whole sky using a camera with a 180-degree (fish-eye) lens and infrared film (For a detailed description of the set-up, operation, and analysis of the photograms see Lund and Shanklin 1972). Along with the photograms, observers recorded routine NWS cloudiness and sunshine measurements. The study focused on hourly observations of both total and opaque sky to determine the relationship between these parameters and CFLOS probabilities based on the photographs.

Through private conversation with Rapp and Schutz, Lund and Shanklin came up with a formula to estimate CFLOS probabilities:

$$CFLOS(\alpha) = \sum_{k=0}^{10} C(\alpha,k)P(k) \qquad (1)$$

where α is the viewing angle, $C(\alpha,k)$ is the probability of a cloud-free line-of-sight at angle α and k tenths cloudiness, and $P(k)$ is the probability of k tenths cloudiness. The photogrammetric data was used to produce relative frequency amounts of cloud-free line-of-sight as a function of elevation angle and National Weather Service observed total sky cover. A separate chart was also produced using only cases where cumuliform clouds

were present, which could be used in locations where a large fraction of the clouds are cumuliform. The formula accurately reproduced the CFLOS probabilities as analyzed by the whole-sky photographs. However, limitations in the sample size led Lund and Shanklin to subjectively smooth the relative frequency curves and produce curves that could be used in locations throughout the world.

Shortly thereafter, Rapp, Schutz, and Rodriguez of the Rand Corporation published their results for calculating CFLOS. While their approach followed along the same lines as McCabe, they attempted to reduce some of the uncertainties of earlier CFLOS calculations in three areas. First, cloud coverage was treated as a distribution instead of a mean cloud cover. Second, the study incorporated vertical distribution of clouds. Finally, it improved on the estimates made by McCabe and others of relationships among look angle, cloud amount, and CFLOS probability at given ranges (Rapp et al 1973).

McCabe's graph was used to calculate CFLOS probabilities all over the world, but it was discovered that using mean monthly cloud amounts produced unlikely results. CFLOS has a nonlinear relationship with cloud amounts for all but very shallow look angles. Inserting an average cloud amount into the graph is viewed as a poor procedure. For example, if a location had fifteen clear days and fifteen overcast days in a month, both the mean cloudiness and CFLOS probability would be 50 per cent. However, entering 50 per cent mean cloud cover and a look angle of 90-degrees into Figure 2-2 produces a CFLOS probability of 90 per cent. In order to overcome the nonlinearity aspect, CFLOS values for each cloud amount were calculated separately and then computed as an average.

The study also questioned de Bary and Möller's vertical distribution of clouds. As an alternate approach, the Rand Corporation interrogated thirteen years of synoptic data for Columbia, MO through a special set of computer programs. Cloud amount and height were extracted.

In 1971, Shanklin and Landwehr released their report on CFLOS calculations based on the photograms taken at Columbia, MO. One of their tables displayed probabilities of cloud-free lines-of-sight for each tenth sky cover, azimuth, elevation angle, and cloud type. Rapp, Schutz, and Rodriguez extracted the data for all clouds and calculated average CFLOS probabilities for all azimuths (Table 2-1). The data was graphed in order to compare to McCabe's probabilities (Figure 2-3).

Table 2-1. CFLOS Probabilities from Photograms of Columbia, Missouri Based on Cloud Distribution and View Angle.

	View Angle									
Cloud Distribution (Tenths)		10	20	30	40	50	60	70	80	90
	1.0	3.8	5.1	5.9	6.9	7.4	7.7	8.0	8.1	7.8
	0.9	13.6	19.2	23.8	26.4	29.4	31.2	31.6	31.9	30.1
	0.8	21.6	31.7	37.4	41.8	45.4	45.7	46.6	47.5	47.2
	0.7	29.8	42.2	49.1	53.3	56.6	58.5	60.6	61.8	59.6
	0.6	37.2	51.8	59.7	63.8	67.5	69.2	71.0	71.1	71.1
	0.5	47.9	58.8	66.6	70.6	74.2	76.2	76.4	77.4	76.1
	0.4	52.1	67.3	72.9	77.9	80.5	82.2	84.0	84.9	84.4
	0.3	63.8	77.0	81.7	83.7	84.8	86.1	86.4	87.4	87.5
	0.2	74.8	85.4	88.5	91.2	91.8	93.0	93.1	93.2	93.4
	0.1	84.7	90.9	93.2	94.8	95.1	95.0	95.5	95.8	95.9
	0.0	97.0	98.1	98.4	98.7	98.8	98.9	99.0	99.1	98.9

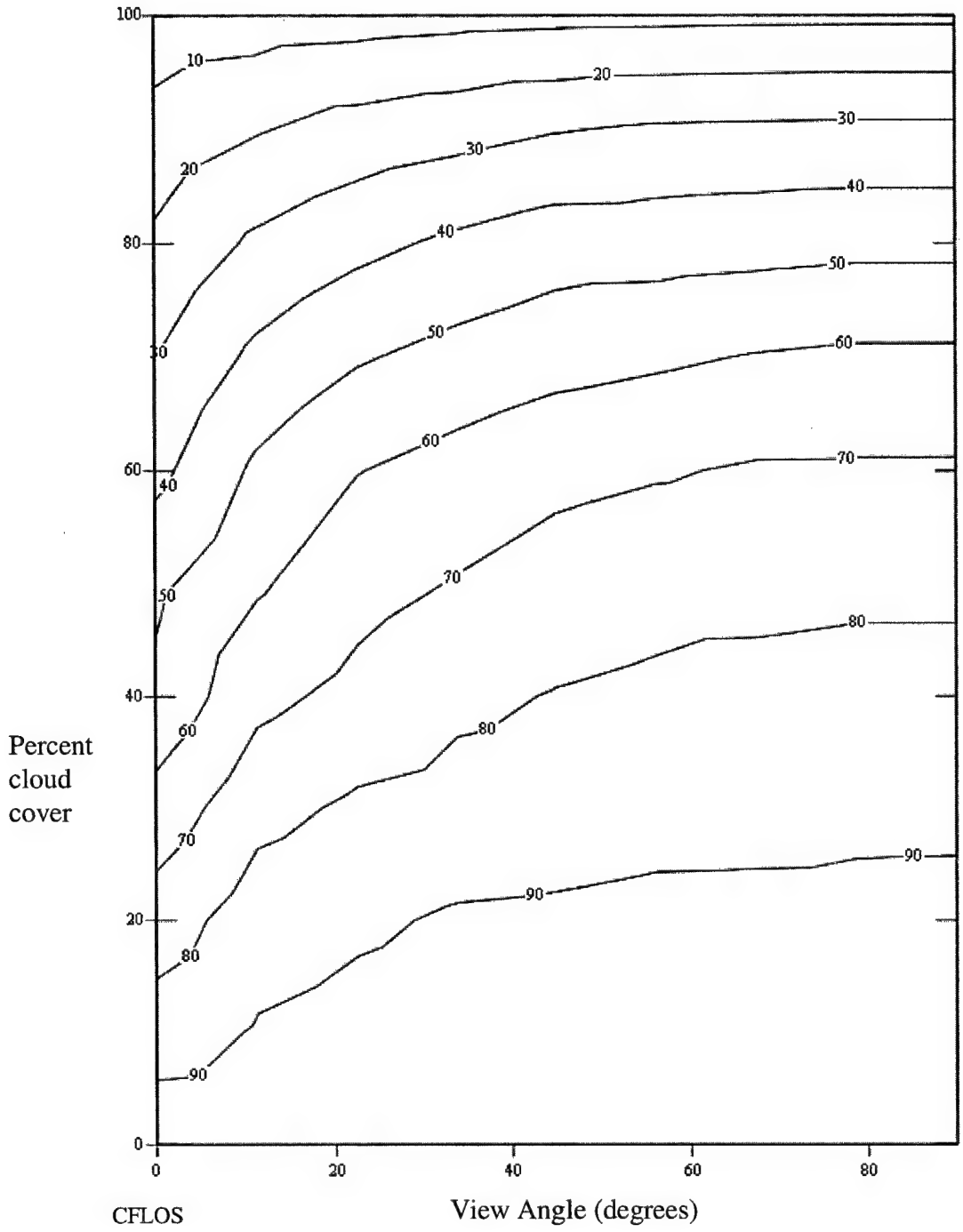

Figure 2-3. Probability of CFLOS for all azimuths and all cloud covers (from Shanklin and Landwehr, 1971, Table 9).

By comparing Figure 2-3 to Table 2-1, one can see the values do not match exactly. The photogram data reaches an unexplained maximum of CFLOS probability before 90 degrees. This seems unrealistic and is probably due either to the way the data were observed, to the effects of lighting at the higher elevation angles, or to both. Therefore, the curves for higher elevation angles were flattened, beginning at the point of highest CFLOS probability (Rapp et al 1973).

Up to this point in the literature timeline, all the CFLOS models relied heavily on the sky coverage as reported by ground observers. In 1979, Malick compared the estimates of cloud cover made by visual observation with those made by photograms. The photographs did not register the presence of thin clouds. Based on his CFLOS probability calculations, Malick transformed the visually indicated sky cover to an integrated sky cover (Table 2-2).

Table 2-2. Transformation of Indicated Sky Cover to Integrated Sky Cover (Linearly interpolated from Malick, 1979).

Indicated Sky Cover (eighths)	Integrated Sky Cover
8/8	0.96
7/8	0.74
6/8	0.61
5/8	0.48
4/8	0.42
3/8	0.32
2/8	0.24
1/8	0.10
0/8	0.04

2.4 MM5

This section will provide a brief background of the MM5 and will discuss some of the general characteristics of the model. For a complete description of MM5, the reader is directed to NCAR/TN-398+STR.

2.4.1 Background

The MM5 is a mesoscale model initially developed by the Pennsylvania State University in 1971. Since that time, the National Center for Atmospheric Research has joined in the ongoing efforts to improve the model, including the fifth generation of the model currently in use, MM5. AFWA began running its version of the model in early 1997.

2.4.2 Model Characteristics

The MM5 generates forecasts valid at 3-hour intervals out to seventy-two hours four times a day with initial analyses valid at 00, 06, 12, and 18 UTC. When available, the model uses the 1° x 1° resolution aviation model for initial and boundary conditions, otherwise the 2.5° x 2.5° resolution Navy Operational Global Analysis and Prediction System data is used. The model uses sigma coordinates to define its vertical coordinate system. Sigma (σ) is a unitless quantity varying from zero to one and is defined by the following relationship of pressures:

$$\sigma = \frac{(p - p_t)}{(p_s - p_t)} \qquad (2)$$

where p is the pressure, p_t is a specified constant top pressure, and p_s is the surface pressure. Figure 2-4 shows an example of a vertical cross section with sixteen full sigma levels (K) and five half-sigma levels. In actuality, the model contains twenty-six full sigma levels and twenty-five half-sigma levels. In this example, the lowest level (K=16) denotes the bottom boundary layer and is terrain following. Physical process parameterizations in the model prescribe such physical processes as surface moisture and heat fluxes along the bottom boundary. The highest level (K=1) corresponds to the top of the boundary and is often considered the tropopause or higher. This quasi-horizontal boundary acts as a material surface limiting the flux of atmospheric properties across it and can be parameterized within the model physics (Pielke 1984).

The MM5 produces forecasts for vertical velocity on the full sigma levels, and forecasts for horizontal wind components, temperature, specific humidity, cloud water, cloud ice, and other prognostic variables. Post processing of the sigma-level forecasts generates forecasts for temperature, relative humidity, vertical velocity, total cloud condensate, and other weather parameters, on various pressure levels.

2.5 Cloud Scene Simulation Model

This section will provide background information towards the development of the Cloud Scene Simulation Model (CSSM) as well as a description of the current program and the input parameters.

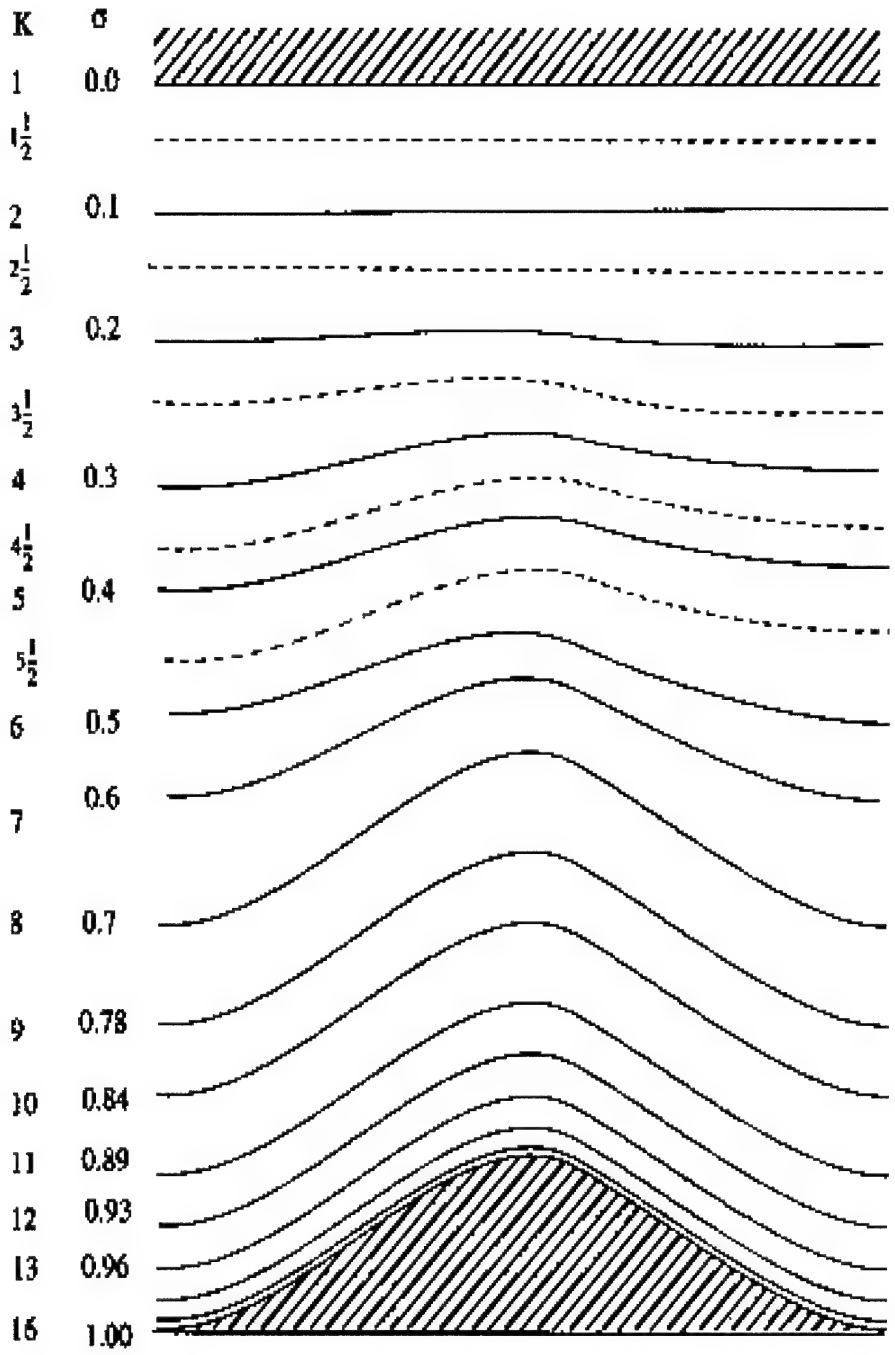

Figure 2-4. Schematic representation of the vertical structure of the MM5 model. Adapted from MMMD/NCAR (MMMD/NCAR 2000).

2.5.1 Background

The Analytical Sciences Corporation in conjunction with the U.S Air Force Phillips Laboratory developed the CSSM for use in the Smart Weapons Operability Enhancement (SWOE) program. A key element of the SWOE program was a planned sensor evaluation and test facility for millimeter wave and infrared data (Cianciolo and Rasmussen 1992). This resulted in a cloud model producing realistic spatial and temporal distributions of cloud water consistent with coarse meteorological input conditions. A list of requirements for the SWOE program is provided in Table 2-3.

Table 2-3. SWOE Cloud Model Requirements.

1. Produce realistic spatial and temporal distributions of cloud water (for stratiform, cirriform, and cumuliform types) in the absence of real data.
2. Treat the complex structure of clouds for realism in radiometric sensor computations (e.g. cloud edge effects).
3. Generate multiple scenes given identical meteorological input for sensitivity studies.
4. Produce cloud fields in a computationally efficient manner.
5. Generate high-resolution cloud fields where necessary for use in radiometric computations and visualization (accommodate low resolution clouds on the horizon).
6. Allow for a wide range of ground domain sizes and resolutions.
7. Provide capability to generate scenes for a variety of sensor applications (e.g. top down, skimmer, air-to-air, etc.).
8. Produce cloud scenes representative of any user-specified location and historical time.
9. Generate model output in a form that can be used for radiometric sensor studies (both MMW and IR applications).
10. Integrate model with other SWOE simulation models
11. Generated cloud shadow map for input to energy balance computations

2.5.2 Model Description

CSSM uses stochastic field generation techniques and knowledge of atmospheric structure to generate up to flour cloud layers (low, middle, high, and cumulus) in four dimensions (three spatial and one temporal). These cloud scenes are statistically representative of specific atmospheric conditions provided by the user including cloud type, layered fractional sky coverage, cloud base and top, temperature, moisture, mean wind speed and direction. A wide variety of cloud types can be modeled, including structured clouds such as cloud streets and wave clouds. Table 2-4 breaks down the cloud types simulated by the CSSM. The program can also accept gridded data to effectively simulate forecast weather conditions provided by the MM5.

Table 2-4. CSSM Simulated Cloud Types.

Cloud Type	**Abbreviation**
Cirrus	Ci
Cirrocumulus	Cc
Cirrostratus	Cs
Cirrus Uncinus	Cn
Stratus	St
Altostratus	As
Nimbostratus	Ns
Stratocumulus	Sc
Altocumulus	Ac
Cumulus	Cu
Precipitating Cumulus	Cp
Stratocumulus Cloud Streets	Scs
Stratus Wave Clouds	Stw

However, CSSM does not precisely model the physical processes within clouds. Such models are extremely expensive, in a computational sense, and are unable to generate cloud fields over a large domain in the minimum time necessary to support real

time simulation and training applications (Kerr 1999). Instead, the stochastic nature of the model generates cloud fields using a core fractal algorithm known as the rescale and add (RSA) algorithm. Briefly put, fractals are shapes having structure at all scales but without a characteristic length. The RSA generates the stochastic cloud fields using a few key model parameters. For example, the variability of liquid water density within cloud elements of differing types is controlled by a "length" parameter selected by an analysis of aircraft-based cloud measurements (Cianciolo and Rasmussen 1996). For a detailed description of fractals and the RSA algorithm, the reader is directed to Kerr, 1999.

2.5.3 CSSM Procedures

This section will highlight the processes used by the CSSM to generate the synthetic cloud fields from the user inputs. For the purpose of this study, the temporal nature of the model was bypassed. For a complete account on the advection of clouds from initialization to a user-specified time, please read Phillips Laboratory Technical Report 96-2079 by Cianciolo, Raffensberger, Schmidt, and Stearns. The discussion will follow the chronological order of the processes common to all cloud types in a stand-alone simulation.

The CSSM begins by processing input sources provided by the user. There are four sources consisting of input parameters, meteorological data, cloud data, and terrain-elevation. The last three can be horizontally homogeneous across the simulation domain.

At this point, the internal working domain must be defined. The size of the CSSM working domain is larger than the user-specified output domain to account for two factors, advection into the output domain and continuity across domain boundaries (interoperability) (Cianciolo and Rasmussen. 1996). Focusing in on the interoperability, several key variables within CSSM are created on a grid box by grid box basis from the coarse, input cloud grid points. These variables are then processed through a bilinear interpolation scheme in order to produce the higher resolution output domain specified by the user. To compute interpolated values near the border of the domain identically, the working domain is expanded by at least one-half of a grid box. Figure 2-5 shows the grid domains used in the CSSM.

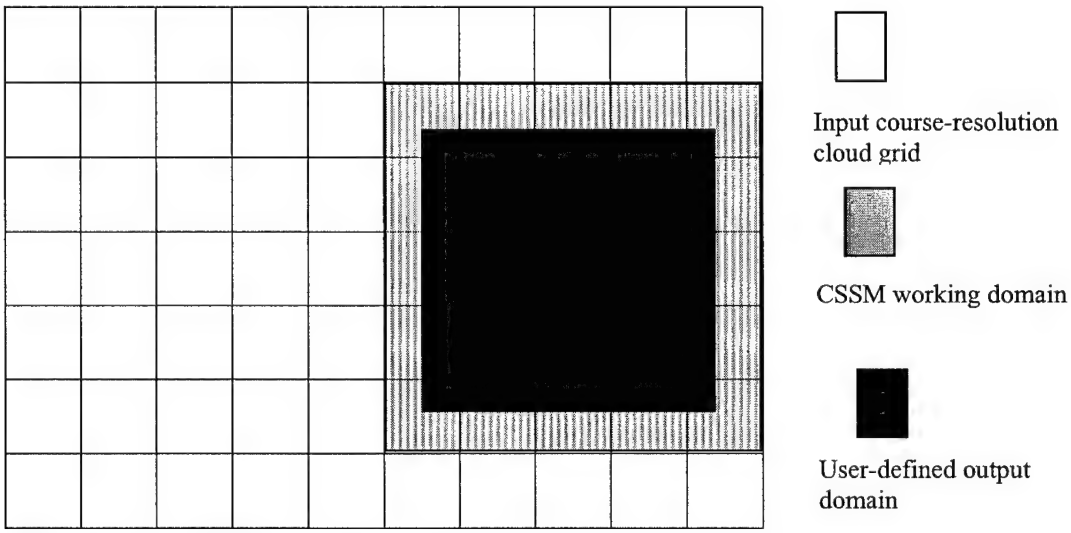

Figure 2-5. CSSM Grid Domains.

When the working domain is defined, the CSSM steps through each input grid box and simulates a cloud field. In order to reduce the amount of data stored in computer memory, the grid boxes are processed one-by-one. All model procedures have been

implemented to ensure data fields are continuous across grid box boundaries (Cianciolo and Rasmussen 1996).

When the working domain is established, the CSSM begins to build the horizontal fractal field. The RSA is employed to provide an efficient point-wise evaluation of the fractal function at every grid point in the working domain. Beginning with Lovejoy's 1982 paper in which he made the case that cloud and rain fields behave as scaling fractals over scales ranging from 1-1000 kilometers, and continuing with Cahalan's analysis of fair weather cumulus, ITCZ clouds, and marine stratocumulus, there is significant evidence that fractal models of cloud structures are appropriate and that many cloud types adhere to either single or multi-fractal scaling laws (Cianciolo and Rasmussen 1996).

After generating the horizontal field, the RSA field values are transformed to a uniform distribution using a standard error function routine. Next, a histogram of the field values is generated and a threshold value is determined for the grid box to produce the desired amount of cloud cover in the box. Each grid box is assigned a threshold value in the first pass through the working domain. These values are then interpolated across the boundaries of all the input grid boxes covering the working domain. A second computational pass is performed and the RSA field values are regenerated, transformed to uniform distribution, and then compared one-by-one to the previous threshold field. All grid point values equal to or greater than the threshold value are determined to be cloud filled, while those less than are set to zero.

2.5.3.1 STRATIFORM CLOUD MODEL

The stratiform cloud model is used to generate cloud fields for all cloud types except cumulus and precipitating cumulus clouds. Three values are calculated, cloud base, cloud height, and water content. The process calculating the bases and height are similar. First, an initial base is interpolated into the working domain from the user-supplied parameters. Next, a perturbation value is calculated in order to account for the irregular bumpiness observed in real clouds. The two values are added together to produce the simulated cloud data. In the case of the cloud tops, the perturbation calculation includes empirical analysis of stratiform cloud data.

The calculation process used above is the same used for the water content. That is, establish a base value, calculate a perturbation value to represent the true state of the atmosphere, and add together to produce the simulated cloud value. In this case, though, the water content calculation is based on the 1974 Feddes synoptic scale model for condensed atmospheric moisture as a function of cloud type and temperature. Grid points with water content values less than two standard deviations from the mean are set to zero. By doing so, small "holes" within the cloud field are established, representative of the true atmosphere.

2.5.3.2 CIRRIFORM CLOUD MODEL

The cirriform cloud model is identical to the stratiform model, but with two additions. First, a non-isotropic horizontal cloud distribution is used to generated clouds with a banded effect. The second addition is a non-isotropic water content structure.

Designed the same way as the stratiform water content, the cirriform model sets all grid points less than one standard deviation below the average to zero. This introduces clear bands within the cloud field, which are frequently observed in nature (Cianciolo and Rasmussen 1996).

2.5.3.3 CUMULIFORM CLOUD MODEL

Beginning with the same horizontal fractal field used in the stratiform model, the cumuliform model converts the field values to a heating field used to initialize the cumulus parcel convection model. At the lifting condensation level, the horizontal field is evaluated and converted to perturbation temperatures. These perturbations are defined with respect to the ambient temperature. Once again, the RSA is called on to define the variability of the heating field. Parcels are then released at random locations across the working domain using a buoyancy determined by the local perturbation temperature. A central finite difference solution to the differential equations that control parcel motion is employed. Mixing with the environmental air is accounted for (where entrainment rates vary as a function of position within the cloud), the water balance is evaluated, and water content is computed for each parcel (Cianciolo and Rasmussen 1996). When the parcels are collected and evaluated, the final step computes an average water content value at each of the output grid points as the average of all overlapping parcels.

III. Methodology

3.1 Background

For the purpose of this study, forecast data from the MM5 in the form of meteograms and gridded output data was used to determine the total fractional cloud amount. During a two-week period in December 2000, meteograms (Figure 3-1) of Sarajevo Bosnia and the corresponding gridded output (Table 3-1) were collected and analyzed, resulting in 63 separate forecast periods. The MM5 shop at AFWA formatted the gridded data in terms of height, temperature, dew point, relative humidity, sky cover, cloud condensate, and reflectivity. Sky cover was produced from two separate tables. The first comes from an Air Weather Service Forecaster Memo, which computed sky cover as a function of the difference between the temperature and the dew point (Table 3-2) (Stock 2000, personal communication). The second computed sky cover as a function of relative humidity and came from AFWA TN-98/002 (Table 3-3).

The meteograms provided a vertical cross-section of the atmosphere in which to evaluate the presence of clouds. Coupled with the gridded output, a subjective analysis of the data could be performed to determine cloud type, bases, tops, layered amounts, and total cloud amounts to be used in the two CFLOS methods.

Bosnia was selected for two reasons. First, it has a high percentage of cloudy conditions in which to evaluate the performance of the two CFLOS methods. Second, it is a region of particular interest for ongoing U.S. military operations. As for the forecast time, the 30-hour forecast was selected because it represented a mission planning forecast window.

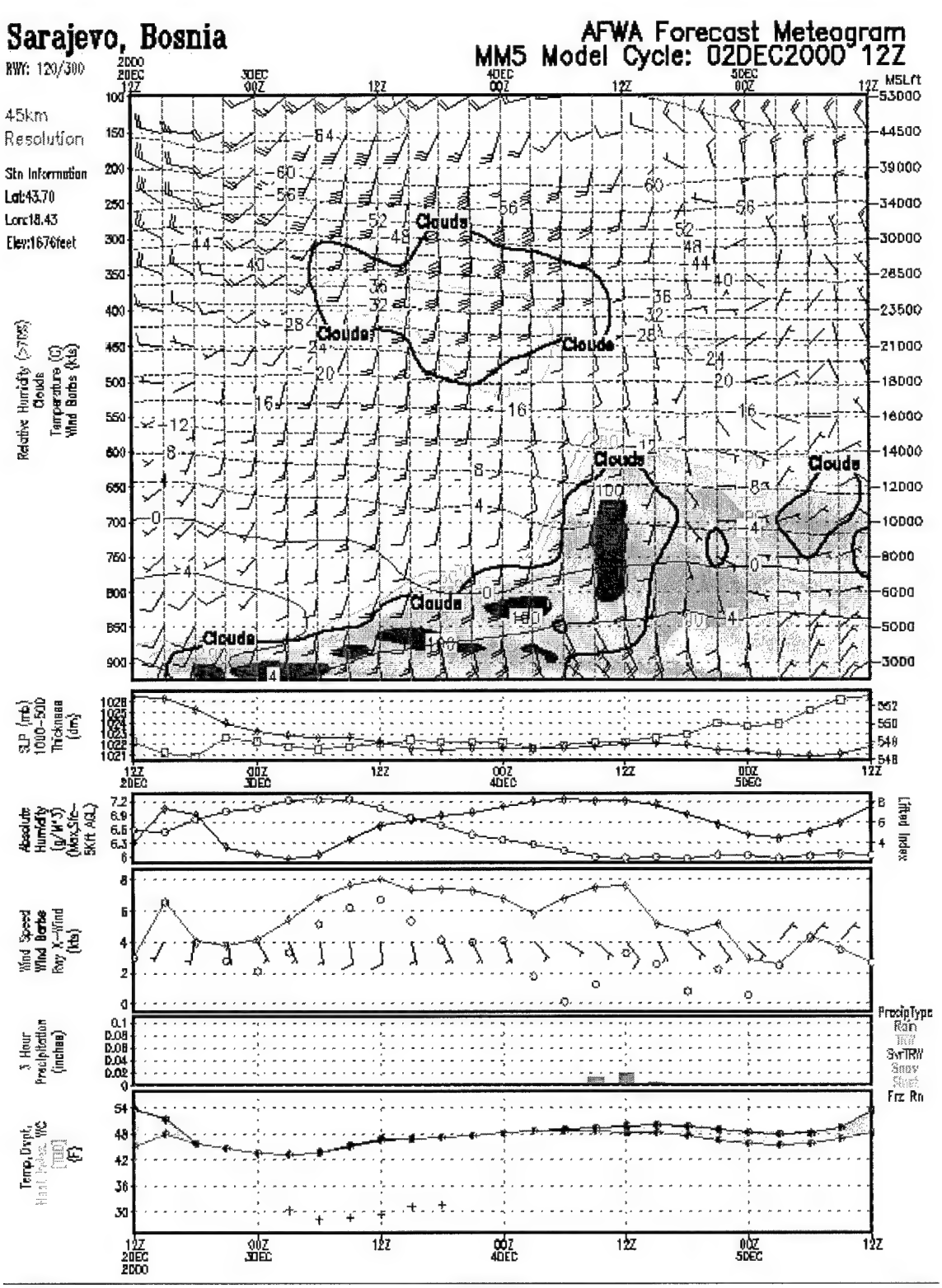

Figure 3-1. Meteogram for Sarajevo, Bosnia.

Table 3-1. Corresponding MM5 gridded output to Figure 3-1.

HEIGHT(ft)	TEMP(c)	DEWPT(c)	RH(%)	PRES(mb)	SKYCVR	CONDSTE (kg/kg)	REFL(dBz)
63.2	4.75	4.37	97.39	897.34	OVC	0.00E+00	0
166.43	4.55	4.29	98.17	893.89	OVC	0.00E+00	0
321.87	4.25	4.17	99.43	888.71	OVC	0.00E+00	0
543.34	3.85	3.85	100	881.38	OVC	4.83E-05	0
832.17	3.35	3.35	100	871.89	OVC	1.14E-04	0
1176.82	2.55	2.55	100	860.67	OVC	1.35E-04	0
1565.54	3.05	1.48	89.38	848.18	OVC	0.00E+00	0
1999.88	2.05	0.74	91.01	834.43	OVC	0.00E+00	0
2481.64	1.65	-0.52	85.46	819.4	BKN	0.00E+00	0
3026.95	1.05	-2.7	76.03	802.67	SCT	0.00E+00	0
3624.6	0.25	-4.7	69.41	784.68	SCT	0.00E+00	0
4292.04	-0.85	-7.1	62.66	765	CLR	0.00E+00	0
5018.49	-1.45	-11.36	47.01	744.06	CLR	0.00E+00	0
5838.5	-2.35	-16.3	33.74	721.04	CLR	0.00E+00	0
6727.41	-3.05	-23.12	19.99	696.81	CLR	0.00E+00	0
7690.63	-4.65	-22.88	23.01	671.37	CLR	0.00E+00	0
8717.62	-6.55	-23.87	24.38	645.09	CLR	0.00E+00	0
9813.98	-8.65	-25.41	25.01	617.98	CLR	0.00E+00	0
10950.01	-11.05	-27.26	25.61	590.86	CLR	0.00E+00	0
12128.98	-13.45	-29.22	25.96	563.73	CLR	0.00E+00	0
13354.62	-16.05	-30.58	28.32	536.59	CLR	0.00E+00	0
14631.13	-18.65	-31.42	32.49	509.45	CLR	1.40E-08	0

Table 3-2. Cloud cover as a function of temperature and dew point.

$T-T_d > 5$ degrees	Clear (CLR)
$T-T_d$ 3-5 degrees	Scattered (SCT)
$T-T_d$ 2-3 degrees	Broken (BKN)
$T-T_d$ 0-2 degrees	Overcast(OVC)

Table 3-3. Cloud cover as a function of relative humidity.

RH %	**Cloud Amount (eighths)**	
<65	0	CLR
70	1 to 2	FEW
75	3 to 4	SCT
80	4 to 5	BKN
85	6 to 7	BKN
>90	8	OVC

3.2 CFLOS Calculations Prescribed by Rapp, Schutz, and Rodriguez

The procedure for calculating a dynamic CFLOS probability based on the method developed at the Rand Corporation is as follows. Instead of using a climatological total fractional cloud amount, the forecast values from MM5 were used. The first step was to perform a multivariate cubic spline interpolation on Table 2-1. In order to do this, view angles of 0 and 100 degrees were added to the table. For a view angle of 0 degrees it is assumed the sensor would never see the ground, hence the CFLOS value is zero for all cloud amounts. The values for an 80-degree view angle were used as the 100-degree values, although it could be argued these values would also be zero. However, it is a moot point because the method does not call for any 100-degree view angles. Table 3-4 shows the modification. MathCAD's® shell for calculating a multivariate cubic spline

Table 3-4. Modified CFLOS Probabilities. Adapted from Shanklin and Landwehr 1971.

	View Angles											
		0	10	20	30	40	50	60	70	80	90	100
Cloud Distribution (Tenths)	0.0	0.0	97.0	98.1	98.4	98.7	98.8	98.9	99.0	99.1	99.1	99.1
	0.1	0.0	84.7	90.9	93.2	94.8	95.1	95.3	95.5	95.8	95.9	95.8
	0.2	0.0	74.8	85.4	88.5	91.2	91.8	93.0	93.1	93.2	93.4	93.2
	0.3	0.0	63.8	77.0	81.7	83.7	84.8	86.1	86.4	87.4	87.5	87.4
	0.4	0.0	52.1	67.3	72.9	77.9	80.5	82.2	84.0	84.9	84.9	84.9
	0.5	0.0	47.9	58.8	66.6	70.6	74.2	76.2	76.4	77.4	77.4	77.4
	0.6	0.0	37.2	51.8	59.7	63.8	67.5	69.2	71.0	71.1	71.1	71.1
	0.7	0.0	29.8	42.2	49.1	53.3	56.6	58.5	60.6	61.8	61.8	61.8
	0.8	0.0	21.6	31.7	37.4	41.8	45.4	45.7	46.6	47.5	47.5	47.5
	0.9	0.0	13.6	19.2	23.8	26.4	29.4	31.2	31.6	31.9	31.9	31.9
	1.0	0.0	3.8	5.1	5.9	6.9	7.4	7.7	8.0	8.1	8.1	8.1

was incorporated for this task

The probability of a cloud-free line-of-sight is calculated using the following equation:

$$PCFLOS_{i,j} := \frac{fit(x_i, cloud_j)}{100} \cdot (1 - cloud)_j \tag{3}$$

where $PCFLOS_{i,j}$ is a two-dimensional matrix of CLFOS probabilities ranging over the various view angles and total fractional cloud amounts, and fit is the MathCAD procedure as a function of view angle and cloud amount based on the modified Shanklin and Landwehr CFLOS table.

3.3 CFLOS Calculations Using the Cloud Scene Simulation Model

CFLOS calculations with this method involved three executable programs and a final process using an Excel spreadsheet. The following will proceed through each program, describing the steps involved. Input files will be displayed in Chapter 4 for each case study.

3.3.1 CSSM

As mentioned earlier, the CSSM requires four input files; a file containing parameters describing the domain, a terrain file, a cloud file, and a meteorological file. The parameter file set the size of the entire domain and grid resolution. This study focused on calculating CFLOS probabilities for an aircraft at five kilometers, therefore the extent of the vertical domain was set at five kilometers. Because the MM5 data had a

45-kilometer grid resolution, the same resolution was reflected in the input file. The model resolution was set to one kilometer by one kilometer by one hundred meters (1km x 1km x 100m) to capture the most cloud elements possible without becoming computationally expensive. Meteorological, terrain, and cloud inputs were chosen to be single values instead of gridded data. In other words, the cloud scene at a single point was horizontally homogeneous across the entire domain. Reasoning for this will be explained in section 3.3.3. Random seed numbers (Table 3-5) were used to develop thirty different cloud scenes for each of the cases in order to determine the variance within the model. Output from this process (water content files) was then moved to the next program.

Table 3-5. Random Seed Numbers for CSSM Input File.

3	5	7	11	13
17	19	23	29	37
41	47	53	59	61
67	71	73	101	91
617	849	1111	2763	3917
4782	5163	6529	7258	8347

3.3.2 Fast Map Postprocessor

The Fast Map postprocessor takes the water content files as inputs and generates optical, radiative, and graphical quantities needed to render realistic three-dimensional cloud images (Kerr 1999). Files containing extinction coefficients at each of the grid points were generated for use in the next program.

3.3.3 Solar Extinction

The solar extinction program computes an integrated extinction coefficient value for a selected path through the domain. The program was significantly modified and simplified from its initial purpose. Initially, the program was designed to track the path of the sun through the day. This called for accurate ephemeris data and complex calculations in order to determine the exact location of the sun or moon. The modified version knows exactly where the aircraft is and the direction of the view angle down to the ground.

First, the domain is reduced five kilometers on each horizontal side to ensure the program does not try to integrate outside the domain. With a working domain of thirty-five by thirty-five by five kilometers, the program moves through the horizontal grid at 5-kilometer increments, maintaining an altitude of 5 kilometers. At each horizontal grid point, the program calculates an integrated extinction coefficient for a view angle of 45 degrees and an azimuthal angle ranging from 1 to 360 degrees. In other words, a 45-degree cone sweeps through the cloud scene at each grid point (Figure 3-2). For each grid point a running count is made of all integrated extinction coefficients less than or equal to 0.0001 to represent a line free of clouds to the ground. The total counts for each point is written to a text file where the data can be further interrogated.

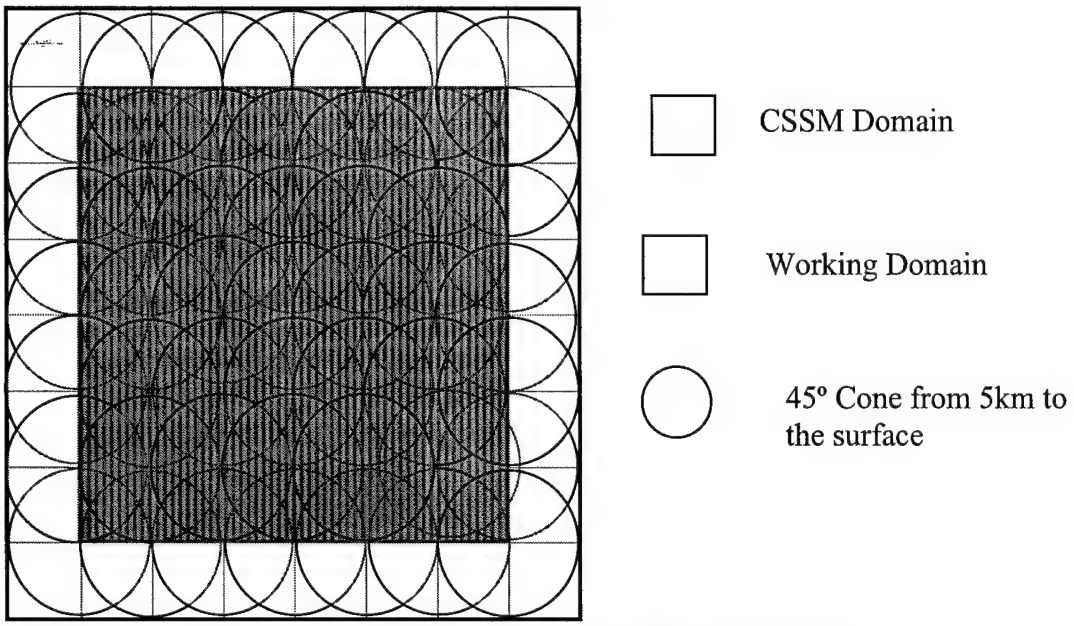

Figure 3-2. Schematic of integrated extinction coefficient coverage.

3.3.4 Final Calculations

When all the total counts (64 values) are written to a file, the data is imported to an Excel spreadsheet in order to calculate the final probabilities. Each total count is divided by 360 to get the CFLOS probability for each grid point. The probabilities are then averaged over the working domain to produce a final CFLOS probability.

3.4 Comparison Data

Data does not exist for verification of CFLOS probabilities. However, analysis of each model's performance can be examined by calculating probabilities based its 90 degree, or nadir, view angle. By looking through the cloud scene straight down, the vertical structure of the clouds is mitigated, reducing the clouds to horizontal, flat sheets.

The procedure for calculating CFLOS probabilities changes slightly for the CSSM process. The azimuthal angles are eliminated and the count values for each point contain either a 1 or 0. In addition, the entire CSSM domain was used, producing 100 grid points instead of 64. In the Excel spreadsheet, the sum of all 100-grid points provides the CFLOS probability. Four different cloud types (stratus, cumulus, stratocumulus, and altocumulus) were independently examined by varying the cloud amount from 5 per cent to 100 per cent in increments of 5 per cent.

IV. Results and Analysis

Four different forecasted cloud files were selected for further examination, each containing a different cloud either type or cloud amount. CFLOS calculations for both methods will be presented and analyzed. Analyzation of all cases will be performed in section 4.5. Section 4.6 will contain the results of the nadir view angle.

4.1 Case 1

Case 1 used the forecast from the 10 December, 2000 at 00 UTC cycle (Figure 4-1 and Table 4-1) and valid at 11 December, 2000 at 06 UTC. A cumulus layer was determined to exist with a base at 98.1 meters and tops of 253.64 meters. The forecasted horizontal distribution was 37.5 per cent. A second layer of altocumulus was forecasted with a base of 2050.51 meters extending up to 4865.64 meters. It contained a horizontal distribution of 37.5 per cent also. The total fractional cloud amount was 62.5 per cent.

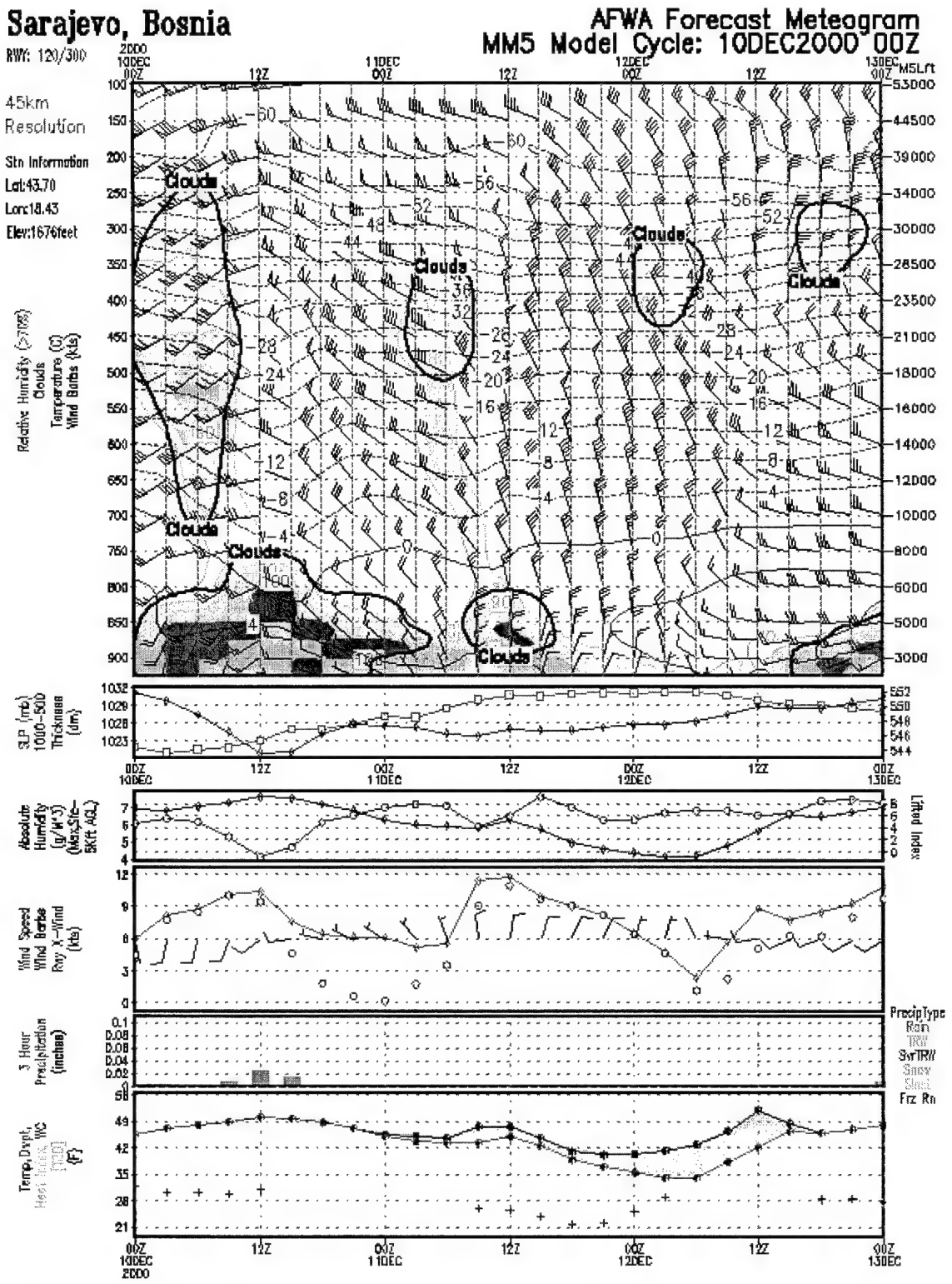

Figure 4-1. Meteogram forecast cycle 10 December 2000 00 UTC.

Table 4-1. MM5 Gridded Output for Figure 4-1.

HEIGHT(ft)	TEMP(c)	DEWPT(c)	RELHUM(%)	PRES(mb)	SKYCVR	CONDSTE (kg/kg)	REFL(dBz)
63.2	8.25	8.07	98.79	900.33	OVC	1.29E-07	0
166.43	8.05	7.99	99.61	896.91	OVC	1.91E-07	0
321.87	7.75	7.75	100	891.79	OVC	4.13E-05	0
543.34	7.35	7.35	100	884.53	OVC	1.14E-04	0
832.17	6.85	6.85	100	875.13	OVC	1.97E-04	0
1176.82	6.15	6.15	100	864.03	OVC	2.67E-04	0
1565.54	5.35	5.35	100	851.64	OVC	3.05E-04	0
1999.88	4.15	4.13	99.85	837.94	OVC	2.71E-04	0
2481.64	3.65	2.26	90.59	822.97	OVC	0.00E+00	0
3026.95	5.85	-3.01	52.9	806.38	CLR	0.00E+00	0
3624.6	6.15	-5.4	43.31	788.65	CLR	0.00E+00	0
4292.04	5.75	-7.99	36.56	769.31	CLR	0.00E+00	0
5018.49	4.85	-8.91	36.24	748.73	CLR	0.00E+00	0
5838.5	2.95	-8.15	43.95	726.06	CLR	0.00E+00	0
6727.41	1.05	-9.03	47.06	702.1	CLR	0.00E+00	0
7690.63	-1.25	-9.26	54.61	676.84	CLR	0.00E+00	0
8717.62	-3.45	-10.87	56.64	650.7	CLR	0.00E+00	0
9813.98	-5.85	-13.23	56.26	623.67	CLR	0.00E+00	0
10950.01	-8.25	-16.17	53.26	596.61	CLR	0.00E+00	0
12128.98	-10.85	-18.54	53.58	569.52	CLR	0.00E+00	0
13354.62	-13.55	-20.19	57.81	542.38	CLR	0.00E+00	0
14631.13	-16.35	-21.87	62.89	515.21	CLR	1.00E-09	0

Table 4-2 shows the input parameter file for the first case. The input parameters are the same for all four cases except for the times. The cloud file is displayed in Table 4-3, while the meteorological inputs are in Table 4-4. Because the inputs are for a single time, the model is not allowed to advect the cloud field horizontally, and the u- and v-wind components are set to zero. The terrain file is the same for all cases and has a single input of 510.8 meters. The resulting CFLOS probability was 23.8 per cent for the first method and 2.7 per cent for the second.

Table 4-2. Input Parameter File for CSSM.

Parameter	Description
2000	/ simulation domain start time: year (1970-2100)
12	/ simulation domain start time: month (1-12)
11	/ simulation domain start time: date (1-31)
06	/ simulation domain start time: hour (0-23)
0	/ simulation domain start time: minute (0-59)
0	/ simulation domain start time: second (0-59)
2000	/ joining domain start time: year (1970-2100)
12	/ joining domain start time: month (1-12)
11	/ joining domain start time: date (1-31)
06	/ joining domain start time: hour (0-23)
0	/ joining domain start time: minute (0-59)
0	/ joining domain start time: second (0-59)
data_cld/chh_cld_	/ root filename of input cloud data
single	/ the word "single" or "grid" specifying the type of input cloud data
2000	/ cloud data start time: year (1970-2100)
12	/ cloud data start time: month (1-12)
11	/ cloud data start time: date (1-31)
06	/ cloud data start time: hour (0-23)
00	/ cloud data start time: minute (0-59)
00	/ cloud data start time: second (0-59)
1.0	/ frequency of input cloud layer files (min) (ignored if #files = 1)
1	/ number of input cloud data files
data_met/chh_met_	/ root filename of input met. data
single	/ the word "single" or "grid" specifying the type of input met data
2000	/ met data start time: year (1970-2100)
12	/ met data start time: month (1-12)
11	/ met data start time: date (1-31)
06	/ met data start time: hour (0-23)
00	/ met data start time: minute (0-59)
00	/ met data start time: second (0-59)
1.0	/ frequency of input met. data files (min) (ignored if #files = 1)
1	/ number of input met data files
data_ter/chh_elev	/ filename of input terrain data
single	/ the word "single" or "grid" specifying the type of input terrain data
output/meso51	/ root name of output files
454848	/ number seed used to initialize fractal
1	/ output gridded water content: 1 = yes, 0 = no
0	/ output precipitation rate: 1 = yes, 0 = no
0	/ interoperability selection: 1 = yes (slower), 0 = no (faster in most cases)
1.0	/ x resolution of output domain (km)
1.0	/ y resolution of output domain (km)
0.1	/ z resolution of output domain (km)
1.0	/ t resolution of output domain (min)
45.0	/ x extent of output domain (km)
45.0	/ y extent of output domain (km)
5.0	/ z extent of output domain (km)
1.0	/ t extent of output domain (min)
0	/ real-time domain origin: 1 = yes, 0 = no
0.0 0.0 0.0 0.0	/ domain origin (x km, y km, z km, t min since joining)

Table 4-3. Cloud File for 11 December, 2000 06 UTC.

Layer	Cloud Type	% Coverage	Base(m)	Top(m)
1	Cumulus	37.5	98.1	253.64
2	Altocumulus	37.5	2050.51	4865.64

Table 4-4. Meteorological Input File for 11 December, 2000 06 UTC.

Pressure(mb)	Height(m)	Temp (°C)	Dew point (°C)	U-Winds(m/s)	V-Winds(m/s)
910.4	510.8	4.2	3.7	0	0
903.5	530.1	3.4	3.1	0	0
900.1	561.5	3.2	2.9	0	0
894.8	608.9	2.9	2.7	0	0
887.4	676.4	2.4	2.3	0	0
877.8	764.4	1.9	1.6	0	0
866.4	869.5	1.9	0	0	0
853.8	988.0	2.5	-2.7	0	0
840	1120.3	2.9	-5	0	0
824.9	1267.2	2.6	-5.9	0	0
808.1	1432.9	1.7	-7.6	0	0
790	1615.6	1	-8.8	0	0
770.2	1819.0	-0.1	-9.9	0	0
749.2	2040.4	-1.2	-11.2	0	0
726	2290.4	-2.6	-10.7	0	0
701.6	2561.3	-4.2	-10.7	0	0
675.9	2854.8	-6.2	-9.5	0	0
649.3	3167.9	-7.8	-9.8	0	0
621.9	3502.1	-9.7	-11.1	0	0
594.6	3848.4	-11.7	-13.1	0	0
567.3	4207.7	-14.1	-15.2	0	0
539.9	4581.3	-16.6	-17.6	0	0
512.5	4970.4	-19.4	-20.3	0	0
485.2	5376.4	-22	-27.4	0	0

4.2 Case 2

Case 2 came from the 7 December, 2000 at 06 UTC cycle (Table 4-5 and Figure 4-2) and valid at 8 December, 2000 at 12 UTC. A layer of stratus was found with a base of 165.1 meters and tops of 253.64 meters. The horizontal distribution was 50 per cent.

Table 4-5. MM5 Gridded Output for Figure 4-3.

HEIGHT(ft)	TEMP(c)	DEWPT(c)	RELHUM(%)	PRES(mb)	SKYCVR	CONDSTE (kg/kg)	REFL(dBz)
63.2	2.25	2.24	99.93	900.63	OVC	2.31E-04	0
166.43	2.05	2.05	100	897.13	OVC	2.72E-04	0
321.87	1.85	1.81	99.72	891.88	OVC	3.40E-04	0
543.34	0.95	0.95	100	884.45	OVC	5.13E-04	0
832.17	6.15	2.37	76.61	874.89	SCT	0.00E+00	0
1176.82	5.05	2.13	81.32	863.74	BKN	0.00E+00	0
1565.54	4.65	-0.86	67.41	851.3	CLR	0.00E+00	0
1999.88	4.55	-2.61	59.66	837.59	CLR	0.00E+00	0
2481.64	4.15	-4.19	54.58	822.62	CLR	0.00E+00	0
3026.95	3.35	-4.54	56.24	805.97	CLR	0.00E+00	0
3624.6	2.65	-5.48	55.05	788.06	CLR	0.00E+00	0
4292.04	1.85	-7.76	48.99	768.47	CLR	0.00E+00	0
5018.49	1.05	-10.59	41.64	747.63	CLR	0.00E+00	0
5838.5	-0.05	-15.06	31.55	724.7	CLR	0.00E+00	0
6727.41	-1.25	-20.77	21.42	700.54	CLR	0.00E+00	0
7690.63	-2.85	-25.82	15.55	675.12	CLR	0.00E+00	0
8717.62	-4.65	-28.43	14.07	648.88	CLR	0.00E+00	0
9813.98	-6.75	-30.57	13.57	621.79	CLR	0.00E+00	0
10950.01	-8.95	-33.92	11.77	594.7	CLR	0.00E+00	0
12128.98	-11.15	-38.29	9.17	567.61	CLR	0.00E+00	0
13354.62	-13.55	-40.69	8.75	540.52	CLR	0.00E+00	0
14631.13	-16.05	-41.87	9.52	513.44	CLR	0.00E+00	0

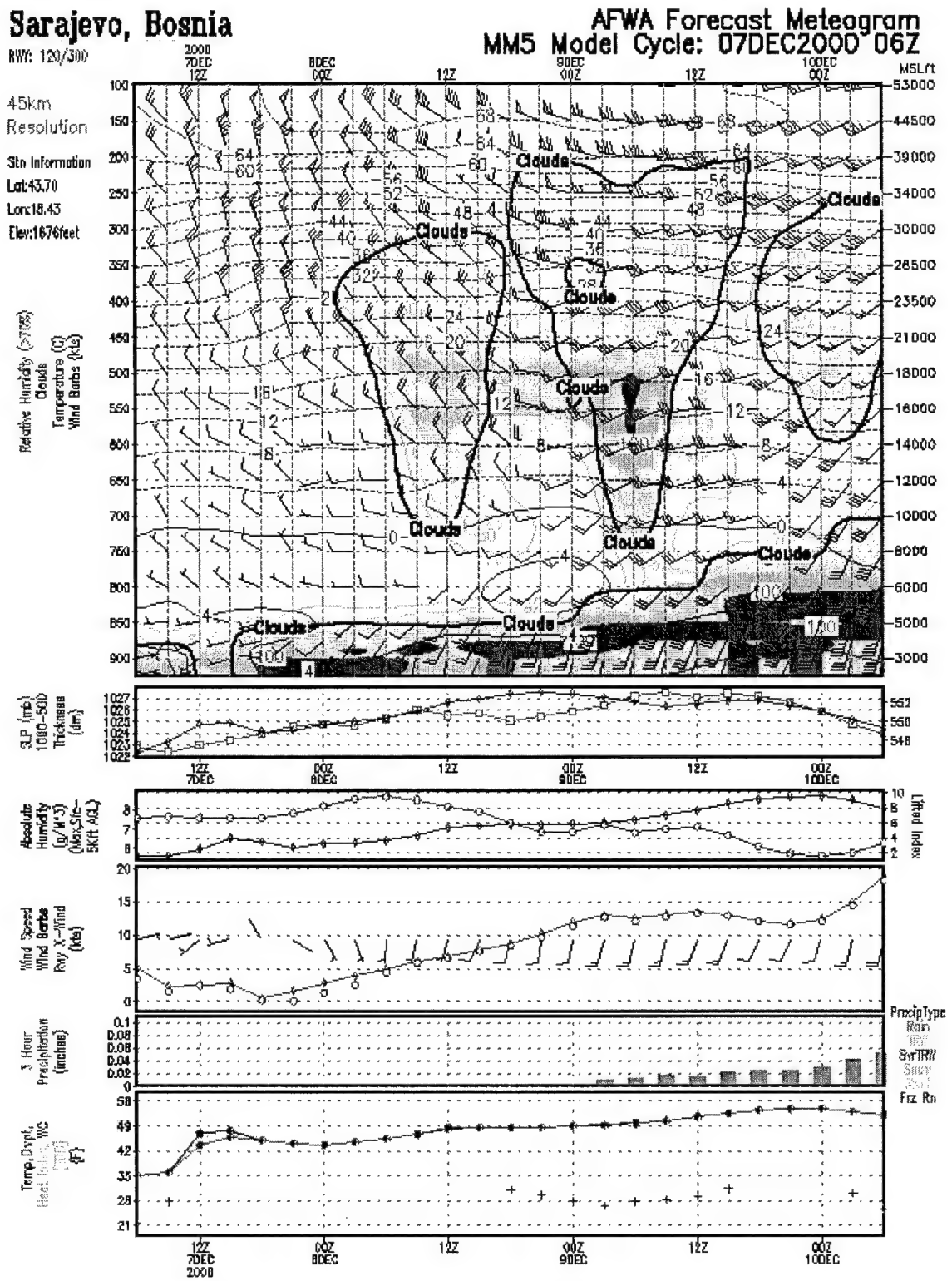

Figure 4-2. Meteogram forecast cycle 7 December 2000 06 UTC.

The cloud file is displayed in Table 4-6, while the meteorological inputs are in Table 4-7. The resulting CFLOS probability was 36.2 per cent for the first method and 36.9 per cent for the second.

Table 4-6. Cloud File for 8 December, 2000 12 UTC.

Layer	Cloud Type	% Coverage	Base(m)	Top(m)
1	Stratus	50.0	165.61	253.64

Table 4-7. Meteorological Input File for 8 December, 2000 12 UTC.

Pressure(mb)	Height(m)	Temp (°C)	Dew point (°C)	U-Winds(m/s)	V-Winds(m/s)
907.4	510.8	7.0	6.0	0	0
901.6	530.1	5.7	5.7	0	0
898.1	561.5	5.5	5.5	0	0
893	608.9	5.3	5.3	0	0
885.6	676.4	4.7	4.7	0	0
876.1	764.4	4.1	4.1	0	0
864.9	869.5	5.9	1.4	0	0
852.5	988.0	8.2	-2.1	0	0
839	1120.3	7.6	-3	0	0
824.1	1267.2	7.4	-4.1	0	0
807.7	1432.9	6.7	-4.4	0	0
789.9	1615.6	5.3	-3.5	0	0
770.4	1819.0	3.7	-2.8	0	0
749.7	2040.4	2.4	-2.5	0	0
726.8	2290.4	0.8	-2.4	0	0
702.7	2561.3	-0.8	-4	0	0
677.3	2854.8	-2.7	-6.2	0	0
651	3167.9	-4.6	-8	0	0
623.9	3502.1	-6.6	-9.8	0	0
596.8	3848.4	-8.6	-11.1	0	0
569.7	4207.7	-10.4	-12.4	0	0
542.6	4581.3	-12.2	-14	0	0
515.6	4970.4	-14.1	-15.6	0	0
488.7	5376.4	-16.1	-17.9	0	0

4.3 Case 3

Case 3 came from the 7 December, 2000 at 12 UTC cycle (Table 4-8) and valid at 8 December, 2000 at 18 UTC. A meteogram was not available. Two cloud layers were forecasted, an overcast stratus layer from 98.1 meters to 253.64 meters, and a scattered altocumulus layer from 3696.91 meters to 4865.64 meters with a horizontal distribution was 25.0 percent.

Table 4-8. MM5 Gridded Output for 30 Hour Forecast 7 December, 2000 12 UTC Cycle.

HEIGHT(ft)	TEMP(c)	DEWPT(c)	RELHUM(%)	PRES(mb)	SKYCVR	CONDSTE (kg/kg)	REFL(dBz)
63.2	5.75	5.72	99.76	901.58	OVC	5.00E-09	0
166.43	5.55	5.54	99.94	898.13	OVC	2.83E-05	0
321.87	5.25	5.25	99.97	892.95	OVC	7.66E-05	0
543.34	4.75	4.75	100	885.6	OVC	1.17E-04	0
832.17	4.05	4.05	100	876.1	OVC	6.68E-05	0
1176.82	5.95	1.39	72.44	864.92	SCT	0.00E+00	0
1565.54	8.15	-2.14	48.14	852.54	CLR	0.00E+00	0
1999.88	7.65	-3	46.75	838.97	CLR	0.00E+00	0
2481.64	7.45	-4.15	43.49	824.15	CLR	0.00E+00	0
3026.95	6.65	-4.39	45.14	807.66	CLR	0.00E+00	0
3624.6	5.25	-3.46	53.34	789.9	CLR	0.00E+00	0
4292.04	3.75	-2.83	62.13	770.43	CLR	0.00E+00	0
5018.49	2.35	-2.46	70.49	749.68	SCT	1.00E-09	0
5838.5	0.85	-2.44	78.64	726.82	SCT	1.00E-09	0
6727.41	-0.85	-4.04	78.97	702.67	SCT	0.00E+00	0
7690.63	-2.65	-6.23	76.45	677.26	SCT	0.00E+00	0
8717.62	-4.55	-8.04	76.69	650.99	SCT	0.00E+00	0
9813.98	-6.55	-9.85	77.5	623.87	SCT	2.50E-08	0
10950.01	-8.55	-11.07	82.13	596.75	BKN	3.31E-07	0
12128.98	-10.45	-12.39	85.8	569.66	OVC	1.40E-06	0
13354.62	-12.25	-14.05	86.6	542.62	OVC	3.37E-06	0
14631.13	-14.05	-15.62	88.04	515.63	OVC	4.18E-06	0

The cloud file is displayed in Table 4-9, while the meteorological inputs are in Table 4-10. The resulting CFLOS probability was 0 per cent for the first method and 10.5 per cent for the second.

Table 4-9. Cloud File for 8 December, 2000 18 UTC.

Layer	Cloud Type	% Coverage	Base(m)	Top(m)
1	Stratus	100.0	98.1	253.64
2	Altocumulus	25.0	3696.91	4865.64

Table 4-10. Meteorological Input File for 8 December, 2000 18 UTC.

Pressure(mb)	Height(m)	Temp (°C)	Dew point (°C)	U-Winds(m/s)	V-Winds(m/s)
913.7	510.8	5	3.8	0	0
905.1	530.1	3.6	1.8	0	0
901.6	561.5	4.2	1.5	0	0
896.3	608.9	4.6	1	0	0
889	676.4	4.4	0.4	0	0
879.4	764.4	3.9	-0.3	0	0
868.1	869.5	3.3	-0.8	0	0
855.5	988.0	2.6	-0.7	0	0
841.6	1120.3	1.9	-0.6	0	0
826.4	1267.2	1.2	-0.6	0	0
809.6	1432.9	0.5	-0.9	0	0
791.4	1615.6	-0.2	-1.5	0	0
771.5	1819.0	-1	-2.5	0	0
750.4	2040.4	-2	-3.7	0	0
727.2	2290.4	-3.3	-5.1	0	0
702.6	2561.3	-4.6	-6.6	0	0
676.9	2854.8	-6	-8.4	0	0
650.3	3167.9	-4.5	-10.9	0	0
623	3502.1	-9.2	-13.7	0	0
595.6	3848.4	-11.1	-17	0	0
568.3	4207.7	-13.3	-20.6	0	0
541	4581.3	-16	-23.4	0	0
513.6	4970.4	-19	-27.1	0	0
486.2	5376.4	-22.4	-30.3	0	0

4.4 Case 4

Case 4 used the forecast from the 10 December, 2000 at 12 UTC cycle (Table 4-11 and Figure 4-3) and valid at 11 December, 2000 at 18 UTC. A thick layer of cumulus was forecasted with its base at 756.4 meters and tops of 2050.51 meters. The forecasted horizontal distribution was 37.5 per cent.

Table 4-11. MM5 Gridded Output for Figure 4-8.

HEIGHT(ft)	TEMP(c)	DEWPT(c)	RELHUM(%)	PRES(mb)	SKYCVR	CONDSTE (kg/kg)	REFL(dBz)
63.2	3.55	1.81	88.35	905.06	OVC	0.00E+00	0
166.43	4.25	1.52	82.35	901.57	BKN	0.00E+00	0
321.87	4.65	1.02	77.25	896.34	SCT	0.00E+00	0
543.34	4.45	0.4	74.88	888.96	SCT	0.00E+00	0
832.17	3.95	-0.31	73.71	879.4	SCT	0.00E+00	0
1176.82	3.35	-0.76	74.43	868.11	SCT	0.00E+00	0
1565.54	2.65	-0.7	78.54	855.51	SCT	0.00E+00	0
1999.88	1.95	-0.55	83.49	841.62	BKN	0.00E+00	0
2481.64	1.25	-0.55	87.76	826.44	OVC	1.00E-09	0
3026.95	0.55	-0.89	90.07	809.55	OVC	6.00E-09	0
3624.6	-0.15	-1.54	90.37	791.39	OVC	2.10E-08	0
4292.04	-0.95	-2.48	89.36	771.53	OVC	5.40E-08	0
5018.49	-1.95	-3.67	88	750.41	OVC	9.50E-08	0
5838.5	-3.25	-5.07	87.26	727.16	OVC	6.90E-08	0
6727.41	-4.55	-6.57	85.85	702.65	BKN	4.20E-08	0
7690.63	-5.95	-8.43	82.71	676.89	BKN	2.00E-09	0
8717.62	-7.45	-10.93	76.32	650.33	SCT	0.00E+00	0
9813.98	-9.15	-13.68	69.88	622.95	SCT	0.00E+00	0
10950.01	-11.05	-17.01	61.83	595.6	CLR	0.00E+00	0
12128.98	-13.25	-20.59	54.55	568.29	CLR	0.00E+00	0
13354.62	-15.95	-23.44	53.15	540.96	CLR	0.00E+00	0
14631.13	-18.95	-27.07	49.48	513.6	CLR	1.00E-09	0

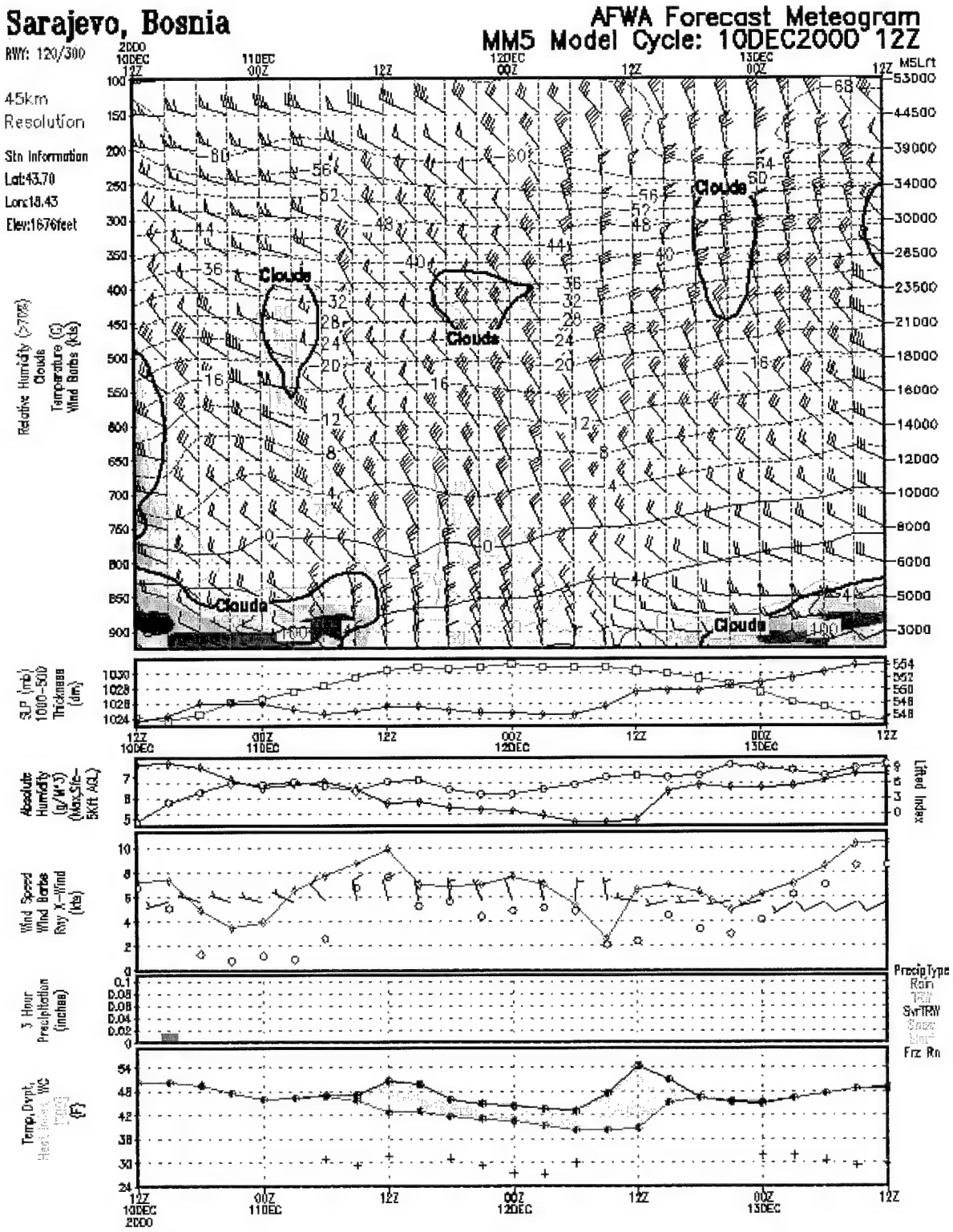

Figure 4-3. Meteogram forecast cycle 10 December 2000 12 UTC.

The cloud file is displayed in Table 4-12, while the meteorological inputs are in Table 4-13. The resulting CFLOS probability was 50.4 per cent for the first method and 13.4 per cent for the second.

Table 4-12. Cloud File for 11 December, 2000 18 UTC.

Layer	Cloud Type	% Coverage	Base(m)	Top(m)
1	Cumulus	37.5	756.4	2050.51

Table 4-13. Meteorological Input File for 11 December, 2000 18 UTC.

Pressure(mb)	Height(m)	Temp (°C)	Dew point (°C)	U-Winds(m/s)	V-Winds(m/s)
913.7	510.8	5	3.8	0	0
905.1	530.1	3.6	1.8	0	0
901.6	561.5	4.2	1.5	0	0
896.3	608.9	4.6	1	0	0
889	676.4	4.4	0.4	0	0
879.4	764.4	3.9	-0.3	0	0
868.1	869.5	3.3	-0.8	0	0
855.5	988.0	2.6	-0.7	0	0
841.6	1120.3	1.9	-0.6	0	0
826.4	1267.2	1.2	-0.6	0	0
809.6	1432.9	0.5	-0.9	0	0
791.4	1615.6	-0.2	-1.5	0	0
771.5	1819.0	-1	-2.5	0	0
750.4	2040.4	-2	-3.7	0	0
727.2	2290.4	-3.3	-5.1	0	0
702.6	2561.3	-4.6	-6.6	0	0
676.9	2854.8	-6	-8.4	0	0
650.3	3167.9	-4.5	-10.9	0	0
623	3502.1	-9.2	-13.7	0	0
595.6	3848.4	-11.1	-17	0	0
568.3	4207.7	-13.3	-20.6	0	0
541	4581.3	-16	-23.4	0	0
513.6	4970.4	-19	-27.1	0	0
486.2	5376.4	-22.4	-30.3	0	0

4.5 Nadir

In order to determine how well each model is performing, consider how each model performs when using a nadir angle.

4.5.1 Method 1 Results

Table 4-14 displays the CFLOS probabilities for the Rapp, Schutz, and Rodriguez procedure when varying the cloud amount. Recall this method averages all cloud types in its calculations. Figure 4-4 is a visual comparison of Method 1 to the actual probabilities.

Table 4-14. Rapp, Schutz, and Rodriguez CFLOS Probabilities at Nadir.

Cloud Amount (%)	True CFLOS Probabilities(%)	Method 1 CFLOS Probabilities(%)
5	95	92
10	90	86
15	85	81
20	80	75
25	75	68
30	70	61
35	65	56
40	60	51
45	55	45
50	50	39
55	45	33
60	40	28
65	35	23
70	30	19
75	25	14
80	20	9
85	15	6
90	10	3
95	5	1
100	0	0

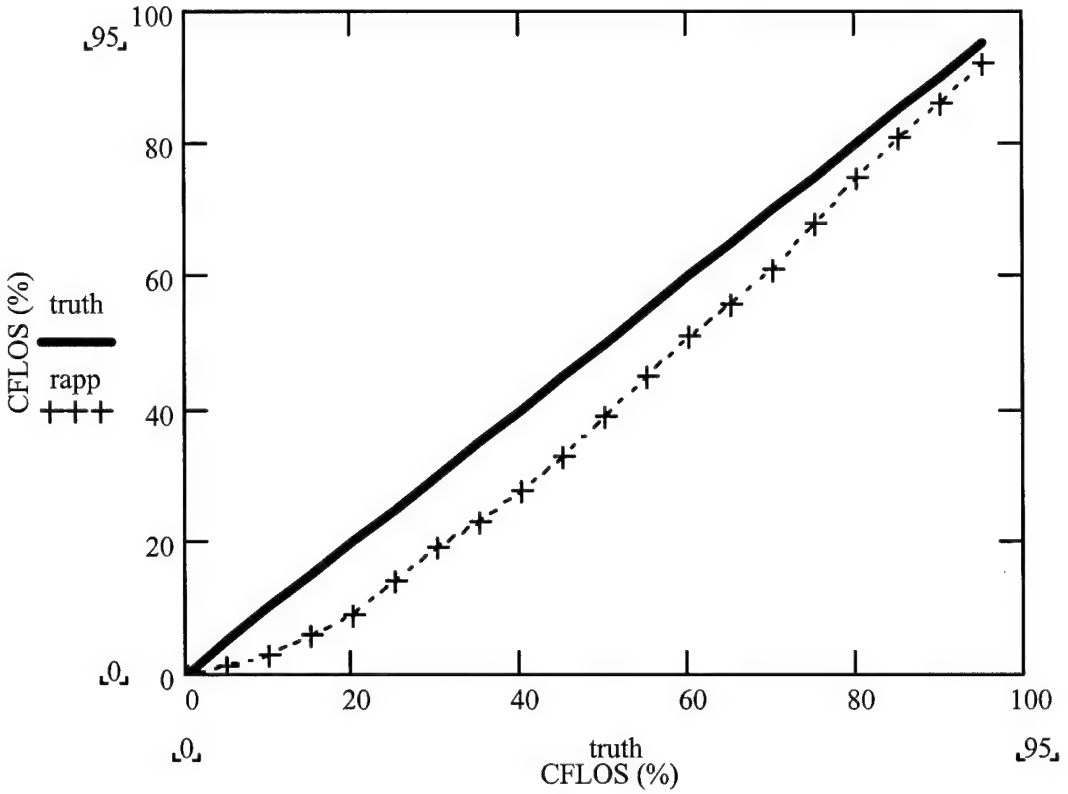

Figure 4-4. Method 1 CFLOS Probabilities vs. Actual CFLOS Probabilities at Nadir.

4.5.2 Method 2 Results

Table 4-15 displays the CFLOS probabilities for each cloud type (stratus, cumulus, stratocumulus, and altocumulus) for the varying cloud amounts at nadir. Figures 4-5 through 4-8 are visual comparisons of each cloud type versus the actual probabilities.

Table 4-15. CFLOS Probabilities for Different Cloud Types.

Cloud Amount(%)	True CFLOS Probabilities(%)	ST(%)	SC(%)	CU(%)	AC(%)
5	95	92	91	79	90
10	90	86	85	68	80
15	85	83	79	49	73
20	80	80	76	38	66
25	75	75	71	30	60
30	70	69	67	28	60
35	65	66	62	22	52
40	60	64	60	17	47
45	55	61	54	15	43
50	50	58	50	14	37
55	45	55	45	9	31
60	40	49	40	7	27
65	35	48	36	7	25
70	30	43	30	5	21
75	25	41	30	4	18
80	20	34	25	2	13
85	15	31	21	1	10
90	10	28	19	0	8
95	5	27	19	0	8
100	0	26	17	0	6

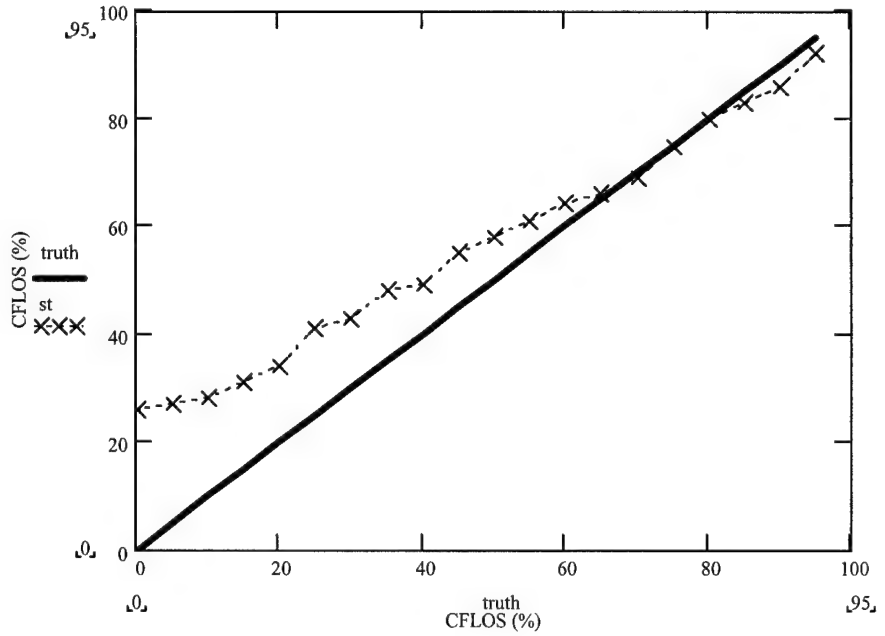

Figure 4-5. Stratus CFLOS Probabilities vs. Actual CFLOS Probabilities at Nadir.

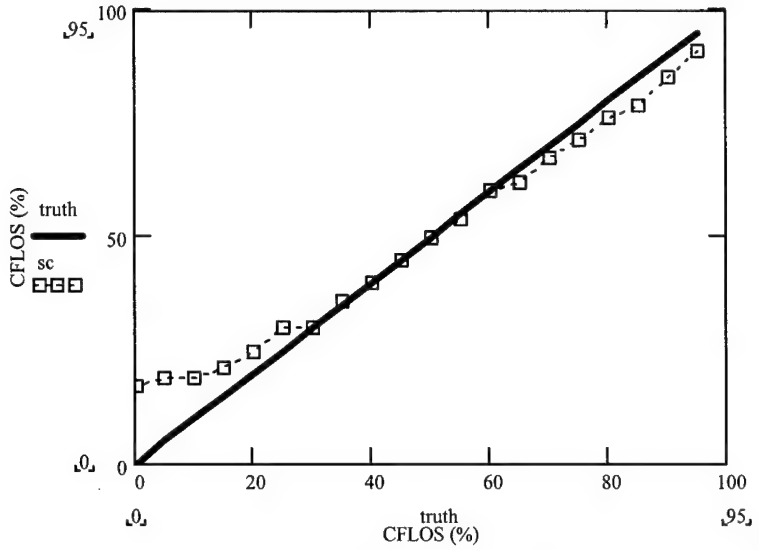

Figure 4-6. Stratocumulus CFLOS Probabilities vs. Actual CFLOS Probabilities at Nadir.

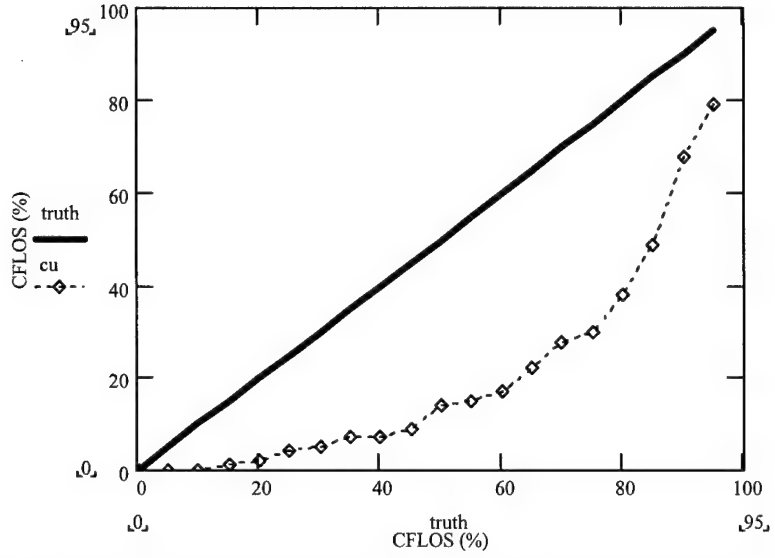

Figure 4-7. Cumulus CFLOS Probabilities vs. Actual CFLOS Probabilities at Nadir.

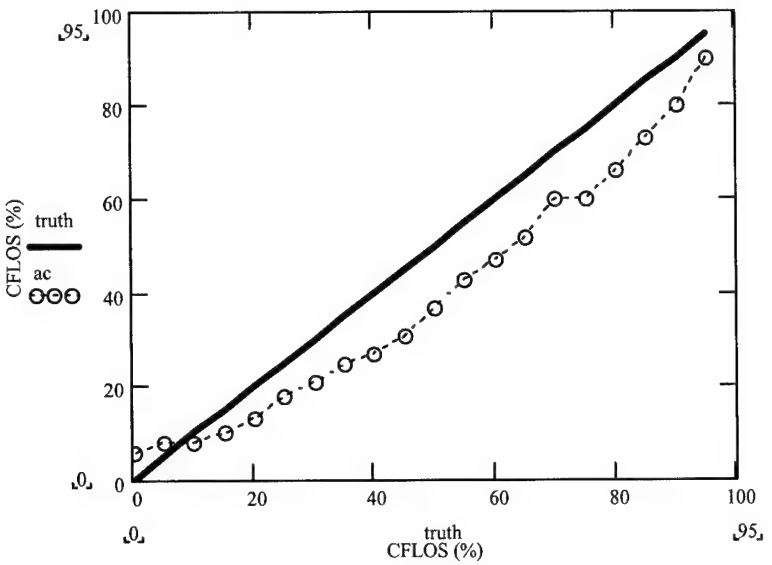

Figure 4-8. Altocumulus CFLOS Probabilities vs. Actual CFLOS Probabilities at Nadir.

4.6 Analysis of Results

Table 4-16 displays the CFLOS probabilities for both methods. Sections 4.6.1 through 4.6.4 will discuss the case studies individually. Section 4.6.5 will analyze the nadir results.

Table 4-16. CFLOS Probabilities.

	Case 1	Case 2	Case 3	Case 4
Method 1	23.8%	36.2%	0%	50.4%
Method 2	2.7%	35.9%	10.5%	13.4%

4.6.1 Case 1

In Case 1, there is a significant cumulus cloud layer (approximately 2800 meters thick) at flight level. Even though it only covers 37.5 per cent of the domain, it will still

reduce most view angles. Another layer at the lower level would further reduce the CFLOS probability

4.6.2 Case 2

Case 2 is a thin stratified cloud layer covering 50 per cent of the domain. Similar probabilities are produced by both methods.

4.6.3 Case 3

Case three displays the results with a completely overcast layer in the low levels and a scattered altocumulus layer at flight level. Method 1 produces the expected result, there is 0 per cent probability of CFLOS though the overcast layer. However, once again the CSSM model does not perform as expected and produces a 10.5 per cent probability through this cloud scene.

4.6.4 Case 4

Case 4 contained a thick cumulus field in the middle of the domain. While the first method produced a highly representative probability, the CSSM model developed a larger horizontal cumulus field than was intended and underestimated a sensible value.

4.6.5 Nadir Look Angle

By examining the performance of each method utilizing the nadir look angle, one might begin to draw some viable conclusions. Figure 4-9 displays how both methods

compared against the known CFLOS probabilities, with the second method being broken down in the aforementioned cloud types.

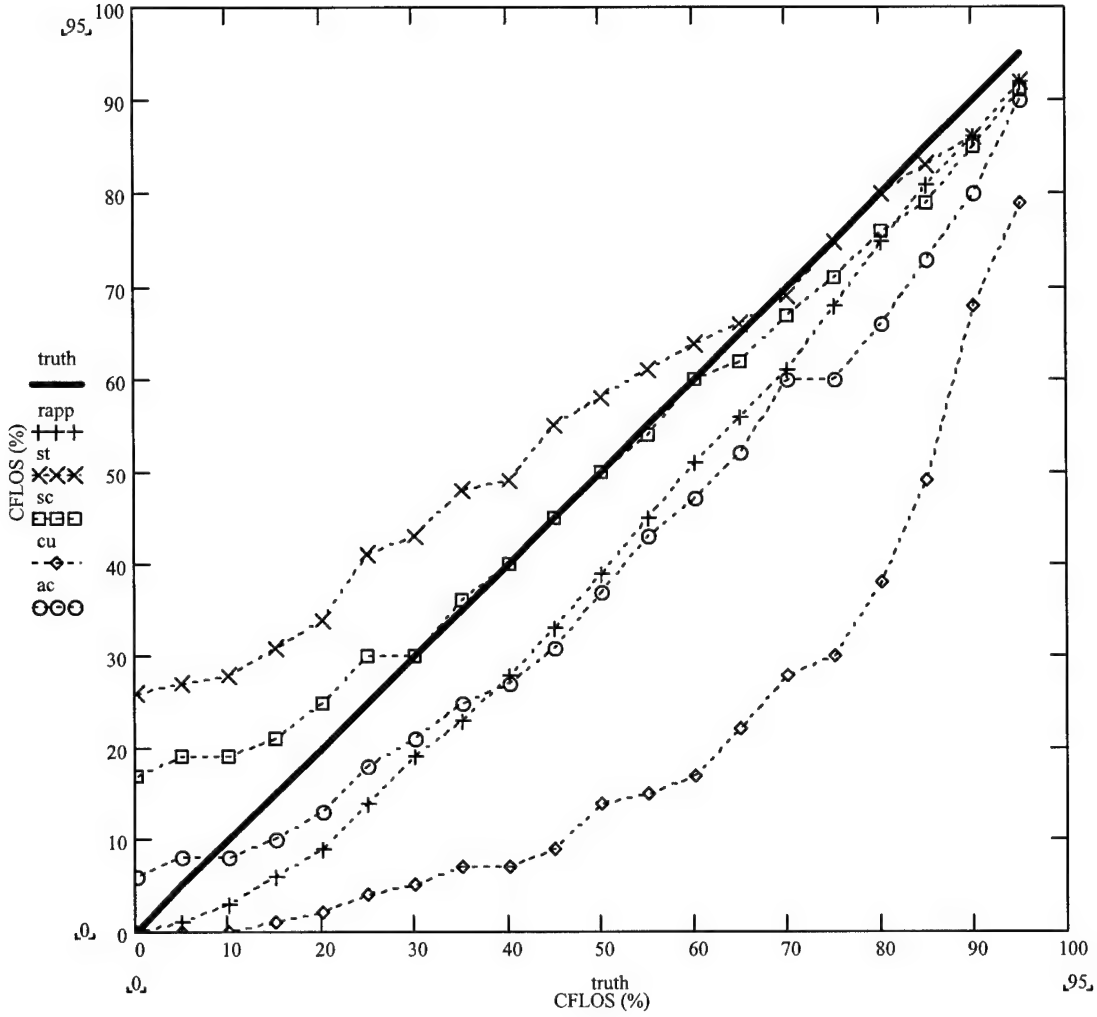

Figure 4-9. CFLOS Probabilities for Methods 1 and 2 vs. Actual Probabilities at Nadir.

It can be seen that the Rapp, Schutz, and Rodriguez procedure underestimates the probabilities for almost all cloud amounts. The exceptions are the small cloud amounts of 0 to 5 per cent horizontal coverage. As for the method using the CSSM, cloud scenes containing cumulus or altocumulus clouds also underestimate the CFLOS probabilities. However, the exceptions for those cloud types are the large cloud amounts of 95 to 100 per cent horizontal coverage. Cloud scenes with stratus clouds greater than 30 per cent horizontal coverage overestimate the CFLOS probabilities. Finally, cloud scenes produced with stratocumulus clouds below 75 per cent horizontal coverage estimated the CFLOS probabilities accurately.

V. Conclusions and Recommendations

The purpose of this study was to identify a process to calculate a CFLOS probability for an aircraft changing in altitude and varying the view angle down to the target. Modifications were made to a previous method to incorporate forecast data and a new method was designed and analyzed. The following summarizes the results.

5.1 Conclusions from the Rapp, Schutz, and Rodriguez Process

At first glance, this method seemed to produce the more realistic CFLOS probabilities for the individual case studies. However, examining its performance with the nadir angle shows a bias of underestimating the actual CFLOS probabilities for almost all horizontal cloud amounts. In general, the underestimation is around 10 per cent for horizontal cloud distributions of 30 to 80 per cent.

5.1.1 Strengths of the Process

The biggest strength of this process is the ease of the calculation. The mathematical process can be easily programmed and a value is quickly returned for any cloud amount or view angle.

5.1.2 Weaknesses in the Process

All the weaknesses associated with the MM5 model are passed along to this process. However, forecasters do not take model data as ground truth, and their

subjective analysis minimizes this consequence. Therefore, the primary weakness lies in the forecast itself.

5.2 Conclusions from Probabilities Calculated Using the CSSM

The probabilities produced using the CSSM model were not consistent with any of the forecasted cloud scenes. Cloud scenes used in the case studies with stratus fared better than those scenes with cumulus and altocumulus. By examining the nadir angles for the four different cloud types, it can be seen that cloud scenes generated by the CSSM with cumulus and altocumulus cloud types severely underestimate the CFLOS probabilities. Cloud scenes produced with stratocumulus clouds produced the most consistent CFLOS probabilities.

5.2.1 Strengths of CSSM Probabilities

The basis for this process was the stochastic method in which the cloud scene was developed. The method used in calculating the integrated solar extinction coefficients worked very well, as did the procedure for actually calculating CFLOS probabilities.

5.2.2 Weaknesses of CSSM Probabilities

The biggest weakness proved to be the over-generation of horizontal clouds for cumulus and altocumulus type clouds. Another factor to consider is the computational expense of running the program. Forecasts with thick cumulus clouds cause the program

to run longer. In addition, the process for marching through the working grid to calculate the probabilities produced a coarse resolution. However, attempts to maximized the resolution caused the program to lock up.

5.3 Implementation of Weather Parameters in AFIT Router Program

In order to implement weather parameters in the AFIT Router program, a Windows-based screen will have to be created for inputs by weather personnel. For UAV operations, these parameters will include areas of turbulence, icing, thunderstorms, CFLOS probabilities over targets, and weather at home station. To use CFLOS probabilities efficiently, threshold probabilities will have to be established for different priority targets. With advancements in cloud analysis and forecast models, these probabilities can be updated during the mission.

5.4 Recommendations for Future Research

The code for the CSSM process needs to be expanded to handle a varying view angle and cruise altitude. In addition, the CSSM code will require some revision to handle the infrared capabilities of the cameras. New methods are constantly being developed and implemented when forecasting clouds, including improvements in types and layered amounts. Studies could also be performed comparing different cloud scene generators. Another possible avenue to pursue is calculating a CFLOS value off observed cloud data and allow it to deteriorate conforming to the Markov process.

Bibliography

"Air Combat Command homepage." Except from unpublished article, n. pag. http://www2.acc.af.mil/library/factsheets/predator.html (1 May 2000).

Air Force Weather Agency. Meteorological Techniques. AFWA TN-98/002. Omaha: HQ AFWA, 15 July 1998.

Air Weather Service, 1992: *T-Twos #3: CFLOS.* Air Weather Service/XTX, 4 pp.

Appleman, H.S., 1962: A comparison of simultaneous aircraft and surface cloud observations. *J. Appl. Meteor.*, **1,** 548-551.

Cahalan, R.F., and J.H. Joseph, 1989: Fractal statistics of cloud fields. *Monthly Weather Review.*, **117**, 261-272.

Cahalan, R.F., 1991: Landsat Observations of Fractal Cloud Structure in Non-Linear Variability, D. Schertzer and S. Lovejoy, Eds., pp. 281-295.

Cianciolo, M.E., and R.G. Rasmussen, 1992: *Cloud Scene Simulation Modeling -- The Enhanced Model*, Technical Report, PL-TR-92-2106, 38pp.

de Bary, E. and Möller, F., 1963: The vertical distribution of clouds. *J. Appl. Meteor.*, **2**, 806-808.

Feddes, R.G., 1974: A Synoptic-Scale Model for Simulating Condensed Atmospheric Moisture, USAFETAC-TN-74-4, 56pp

Kerr, D.G. *A Validation Study of Cloud Scene Simulation Model Temporal Performance.* MS thesis, AFIT/GM/ENP/99M-08. School of Engineering, Air Force Institute of Technology (AU), Wright-Patterson AFB, OH, March 1999.

Lovejoy, S., 1982: Area-perimeter relation for rain and cloud areas, *Science*, **216**, 185-187.

Lund, Iver A., 1966: Methods for estimating the probability of clear lines-of-sight, or sunshine, through the atmosphere. *J. Appl. Meteor.*, **5,** 625-630.

Lund, Iver A. and M. D. Shanklin, 1972: Photogrammetrically determined cloud-free lines-of-sight through the atmosphere. *J. Appl. Meteor.*, **11,** 773-782.

Malick, John D., J. H. Allen, and S. Zakanycz, 1979: Calibrated analytical modeling of cloud-free intervals. *SPIE*, **195,** 142-147.

McCabe, J. T., 1965: Estimating mean cloud and Climatological probability of cloud-free line-of-sight. Tech. Rept. 186, Air Weather Service (MATS), 26 pp.

Mesoscale and Microscale Meteorology Division/National Center for Atmospheric Research. *PSU/NCAR Mesoscale Modeling System Tutorial Class Notes and User's Guide: MM5 Modeling System Version 3.* January 2000.

O'Rourke, Kevin P. *Dynamic Unmanned Aerial Vehicle (UAV) Routing With a Java-Encoded Reactive Tabu Search Metaheuristic.* MS thesis, AFIT/GOA/ENS/99M. School of Engineering, Air Force Institute of Technology (AU), Wright-Patterson AFB OH, February 1999.

Pielke, R. A. *Mesoscale Meteorological Modeling.* Academic Press, 1984. 612 pp.

Pukall, Brian D. *A Comparison of Advect Cloud Model and Fifth-Generation Mesoscale Model Total Fractional Cloud Forecasts.* MS thesis, AFIT/GM/ENP/98M-08. School of Engineering and Management, Air Force Institute of Technology (AU), Wright-Patterson AFB OH, March 1998.

Rapp, R. R., C. Schutz,, and E. Rodriguez, 1973: Cloud-free line-of-sight calculations. *J. Appl. Meteor.*, **12**, 484-493.

Shanklin, M. D., and J.B. Landwehr, 1971: Photogrammetrically determined cloud-free lines-of-sight at Columbia, Missouri. Final Rept., AFCRL-71-0273, Air Force Cambridge Research Laboratories, 185 pp.

Stock, C.M., Captain, USAF, Chief, DNXT Visualization Team, AFWA, Offutt Air Force Base. Personal Correspondence.

Vita

Captain Joseph J. Golemboski III was born in Tulsa, Oklahoma. He graduated as from Bishop Kelley High School in Tulsa in May 1989 and was awarded a partial Air Force Reserve Officer Training Corps scholarship. He entered undergraduate studies at the University of Arizona in Tucson, Arizona. He graduated with a Bachelor of Science degree in Atmospheric Sciences and was concurrently commissioned by Detachment 020 of the University of Arizona in August 1993.

His first assignment was at Osan AB, Republic of Korea, as an assistant staff weather office in October 1993. In October 1994, he was assigned to 57th Operations Support Squadron, Nellis AFB, NV as the wing weather officer. While at Nellis, he was PCA'd into the 11th Reconnaissance Squadron as Chief of Weather in June 1997. He deployed in supported of Predator unmanned aerial vehicle operations in the Balkans, including Operation ALLIED FORCE. In August 1999, he entered the Graduate Meteorology program, Graduate School of Engineering and Management, Air Force Institute of Technology.

J.J. is married to the former Clarissa A. De La Riva of El Paso, Texas. They have three children, Mikayla, Gillian, and Noah.

REPORT DOCUMENTATION PAGE

Form Approved
OMB No. 074-0188

PLEASE DO NOT RETURN YOUR FORM TO THE ABOVE ADDRESS.

1. REPORT DATE *(DD-MM-YYYY)*	2. REPORT TYPE	3. DATES COVERED *(From – To)*
01-16-2001	Master's Thesis	Jun 2000 – Mar 2001

4. TITLE AND SUBTITLE

ANALYSIS OF CLOUD-FREE LINE-OF-SIGHT PROBABILITY CALCULATIONS

5a. CONTRACT NUMBER

5b. GRANT NUMBER

5c. PROGRAM ELEMENT NUMBER

6. AUTHOR(S)

Golemboski, Joseph J. III., Captain, USAF

5d. PROJECT NUMBER
If funded, enter ENR #

5e. TASK NUMBER

5f. WORK UNIT NUMBER

7. PERFORMING ORGANIZATION NAMES(S) AND ADDRESS(S)

Air Force Institute of Technology
Graduate School of Engineering and Management (AFIT/EN)
2950 P Street, Building 640
WPAFB OH 45433-7765

8. PERFORMING ORGANIZATION REPORT NUMBER

AFIT/GM/ENP/01M-03

9. SPONSORING/MONITORING AGENCY NAME(S) AND ADDRESS(ES)

UAV Battlelab
Attn: Lt Col Mark O'Hair
1003 Nomad Way, Suite 107
Eglin AFB, FL 32542-6867 DSN: 872-5940 x208

10. SPONSOR/MONITOR'S ACRONYM(S)

11. SPONSOR/MONITOR'S REPORT NUMBER(S)

12. DISTRIBUTION/AVAILABILITY STATEMENT

APPROVED FOR PUBLIC RELEASE; DISTRIBUTION UNLIMITED.

13. SUPPLEMENTARY NOTES

14. ABSTRACT

Cloud-free line-of-sight probabilities were calculated using two separate methods. The first was a variation of a method developed by the Rand Corporation in 1972. In it, CFLOS probabilities were calculated using empirical data based on five years of photograms taken over Columbia, Missouri and forecasted cloud amounts rather than climatological values. The second was a new approach using the Cloud Scene Simulation Model developed by Phillips Laboratory. Cloud scenes were generated using forecasted cloud fields, meteorological inputs, and thirty random numbers. Water content files were produced and processed through a follow-on program to determine the extinction coefficients at each grid point in the working domain. A reiterative routine was written to integrate the extinction coefficients along a view angle from the top of the domain down to the surface at separate points within the horizontal domain. The values of each point were summed and averaged over the working domain to determine the CFLOS probability for the target area. The nadir look angle was then examined for both methods. Stratus, stratocumulus, cumulus, and altocumulus cloud types were independently examined with the CSSM generated cloud scenes. Each method and cloud type were compared against the known CFLOS probability for nadir. Results indicate the method developed in 1972 underestimates CFLOS probabilities by as much as twelve per cent with horizontal cloud coverage ranging from 30 to 80 per cent. CSSM generated cloud scenes varied depending on the cloud type analyzed, with stratocumulus clouds measuring up the best against the known probabilities.

15. SUBJECT TERMS

Cloud-free line-of-sight (CFLOS), Unmanned Aerial Vehicle (UAV), Predator, Cloud Scene Simulation Model (CSSM), Fifth Generation Mesoscale Model (MM5).

16. SECURITY CLASSIFICATION OF: UNCLASSIFIED			17. LIMITATION OF ABSTRACT	18. NUMBER OF PAGES	19a. NAME OF RESPONSIBLE PERSON
a. REPORT	b. ABSTRACT	c. THIS PAGE			Lt Col Michael K. Walters, ENP
UL	UL	UL	UL	76	19b. TELEPHONE NUMBER *(Include area code)* (937) 255-3636, ext 4681